Modelling spatial dispersion of contaminants from shipping lanes in the Baltic Sea

Marine Pollution Bulletin 173 (2021) 112985

Contents lists available at ScienceDirect

Marine Pollution Bulletin

journal homepage: www.elsevier.com/locate/marpolbul

Modelling spatial dispersion of contaminants from shipping lanes in the Baltic Sea

Ilja Maljutenko [a], Ida-Maja Hassellöv [b], Martin Eriksson [b], Erik Ytreberg [b], Daniel Yngsell [b], Lasse Johansson [c], Jukka-Pekka Jalkanen [c], Mariliis Kõuts [a], Mari-Liis Kasemets [a], Jana Moldanova [d], Kerstin Magnusson [e], Urmas Raudsepp [a,*]

[a] Department of Marine Systems, Tallinn University of Technology, Akadeemia tee 15a, 12618 Tallinn, Estonia
[b] Department of Mechanics and Maritime Sciences, Chalmers University of Technology, Hörselgången 4, 41756 Gothenburg, Sweden
[c] Atmospheric Composition Research, Finnish Meteorological Institute, 00560 Helsinki, Finland
[d] IVL Swedish Environmental Research Institute, 400 14 Gothenburg, Sweden
[e] IVL Swedish Environmental Research Institute, Kristineberg Marine Research, Kristineberg 566, 451 78 Fiskebäckskil, Sweden

ARTICLE INFO

Keywords:
Ship pollution
Ship waste
Water circulation
Vertical mixing
Contaminant dispersion
Baltic Sea

ABSTRACT

Major sources of pollution from shipping to marine environments are antifouling paint residues and discharges of bilge, black, grey and ballast water and scrubber discharge water. The dispersion of copper, zinc, naphthalene, pyrene, and dibromochloromethane have been studied using the Ship Traffic Emission Assessment Model, the General Estuarine Transport Model, and the Eulerian tracer transport model in the Baltic Sea in 2012. Annual loads of the contaminants ranged from 10^{-2} tons for pyrene to 100 s of tons for copper. The dispersion of the contaminants is determined by the surface kinetic energy and vertical stratification at the location of the discharge. The elevated concentration of the contaminants at the surface persists for about two-days and the contaminants are dispersed over the spatial scale of 10-60 km. The Danish Sounds, the southwestern Baltic Sea and the Gulf of Finland are under the heaviest pressure of shipborne contaminants in the Baltic Sea.

1. Introduction

Shipping is a significant source of marine pollution and therefore causes inevitable stress to the marine environment (Andersson et al., 2016). Sardain et al. (2019) project global maritime traffic to increase by 240–1209% by 2050, which intensifies pressures on the environment, while preventive countermeasures are taken by way of more stringent International Maritime Organization (IMO) regulations (Chu Van et al., 2019). Everyday ship operations at sea and maintenance at berth are the significant sources of marine pollutants. They consist of air emission and the subsequent deposition of contaminants at the sea surface, direct discharges to the water, and physical impacts, such as noise and artificial light (Jägerbrand et al., 2019). Direct input of contaminants from ships to the sea, which is the focus of the study, includes leaching of antifouling paint (AFP), discharge of scrubber effluent (SC), ballast water (BA), bilge water (BI), black water (BW) and grey water (GW).

The AFPs are used to reduce biofouling (growth of marine organisms) on ship hulls (Almeida et al., 2007). Biofouling increases vessel resistance since a rough surface increases friction and thereby vessel fuel consumption. The main function of AFPs in the prevention of biofouling is a continuous release of biocides from the paint surface (e.g. Abioye et al., 2019). The AFP market is to some extent controlled by country-specific regulations (e.g. Thomas and Brooks, 2010) as well as international conventions (IMO, 2001). In addition, leisure boats contribute to the release of AFP biocides during movement and mooring, mainly in the coastal and archipelago areas (Johansson et al., 2020).

Exhaust gas cleaning systems, also known as scrubbers, are used to reduce emissions of sulphur oxides to the atmosphere as an alternative option to comply with the maximum allowed fuel sulphur content for vessels operating in different regions (Merico et al., 2021). From January 2020, stricter global regulations on the maximum allowed sulphur content in marine fuels apply, which has led to a substantial increase in scrubber installations since 2017 (DNV-GL, 2020). Currently, there are also five Sulphur Emission Control Areas (SECA) enforced by MARPOL Annex VI and several other areas set up by national or regional legislation (Endres et al., 2018). The chemical composition of scrubber

* Corresponding author.
E-mail address: urmas.raudsepp@taltech.ee (U. Raudsepp).

https://doi.org/10.1016/j.marpolbul.2021.112985
Received 27 April 2021; Received in revised form 16 September 2021; Accepted 17 September 2021
Available online 28 September 2021

effluents is highly variable and there is increasing concern about the environmental impact from wide-scale use of scrubbers (Endres et al., 2018; Hassellöv et al., 2020).

Geographical redistribution of water masses via BA discharge from ships can evoke multiple ecological risks (Endresen et al., 2004), including invasion of non-indigenous species (Kernan, 2015), water pollution with heavy metals (Feng et al., 2017) and microplastics (Naik et al., 2019), redistribution of toxin-producing algae (Cheniti et al., 2018), and the introduction of new pathogens and diseases to the surrounding medium (Ruiz et al., 2000; Altug et al., 2012). Common legislation acts (IMO, 2004) have been developed and put into action for BA treatment to reduce those risks (David and Gollasch, 2008; Werschkun et al., 2014). The Ballast Water Management convention (IMO, 2004) requires ballast water to be treated prior to discharge to reduce the risk of introducing non-indigenous species. However, these required ballast water management systems have been identified as a new source of contaminants, as they use biocides and can create disinfection bi-products that are released to the marine environment (Delacroix et al., 2013).

BI is mainly condensed water from machinery spaces containing oily water, cleaning agents and metals (Magnusson et al., 2018). BI may be directly discharged to the marine environment from ships en route only if it contains less than 15 ppm oil (IMO, 2011). About 75% of treated BI is discharged to the sea (Det Norske Veritas, 2009), which amounts to 270,000 tons per year globally and is comparable to a single major oil spill (Tiselius and Magnusson, 2017; Farrington, 2013). The toxicity of BI to the marine environment varies depending on the mixture of different surfactants and oils (Greer et al., 2012) carried on board. Magnusson et al. (2018) showed that the pollutants from BI had persistently elevated concentrations in shipping lanes, but the concentrations were 4 to 8 orders of magnitude below known toxic levels.

BW contains any contaminants from toilets and urinals, wash water from medical premises and spaces containing living animals (Lindgren et al., 2016). GW is defined as drainage from dishwater, showers, laundry, baths and washbasins (Ytreberg et al., 2020). BW mainly discharges nutrients (Lindgren et al., 2016; Wilewska-Bien et al., 2019), the impact of which on the marine environment is accounted through biogeochemical cycling (Raudsepp et al., 2013, 2019). Contaminants of environmental concern in BW include metals, pharmaceuticals and other organic compounds. Detergents, disinfectants, pharmaceuticals and personal care products are contributors in GW (Ytreberg et al., 2020). The amount of BW and GW discharge depends on the type of vessel. Fishing and passenger vessels are the main contributors (Parks et al., 2019) because their waste streams are connected to the large number of people carried on board.

There is continuous research on the release of copper and zinc from antifouling paints, their toxicity and environmental impact. Recently, a capability of the X-Ray Fluorescence method for in situ detection of environmental release rates of metallic or organometallic biocides has been shown (Lagerström and Ytreberg, 2021). AFP particles have been recognized as important marine microplastic pollution (Gaylarde et al., 2021; Torres and De-la-Torre, 2021), which has led to the synthesis of ecofriendly antifouling paints (Kyei et al., 2020). The research on the discharge of contaminants to the sea by open loop scrubbers has advanced in recent years. Despite the reduction of sulphur emission to the air, the implementation of open loop scrubbers may introduce a considerable amount of pollutants to the sea, which may cancel the positive effect of the implementation of scrubbers on air quality (Hermansson et al., 2021; Claremar et al., 2017; Turner et al., 2017). This has initiated a number of studies on the impact of scrubber water discharge on marine ecology (Koski et al., 2017; Teuchies et al., 2020; Ytreberg et al., 2019; Thor et al., 2021). Moldanová et al. (2021) have proposed a holistic approach for the assessment of ship traffic related pressures on marine environment and air quality, their impact on biota and human health.

The area impacted by shipborne pollutants depends on the spatio-temporal distribution of the load and dispersion of contaminants in the marine environment (Jalkanen et al., 2021). Qualitatively, the spatio-temporal distribution of the loads can be estimated by taking into consideration vessel activity data and international and national regulations. Quantitative estimations of the chemical composition and volumes of discharges is a challenging task. The amount of the load depends on vessel type, the engines, and number of crew and passengers on board. Chemical composition is dependent on the factors listed above and types and amounts of the chemicals used onboard.

The patterns of contaminant input show the marine areas with the highest concentrations of contaminants and a direct impact on marine organisms. The most dynamic layer of the sea is the surface layer where waves, Stokes drift, wind-driven currents, and vertical mixing can disperse discharged contaminants over much larger areas than the source region. Surface circulation along with vertical dispersion spread the contaminants over areas in the biologically active euphotic zone where the impact of pollution is the most immediate. Below the energetic surface layer, contaminants are dispersed by more persistent water currents. The contaminants adsorb to the settling particles and accumulate in the sediments. There, physicochemical and biogeochemical processes may release the contaminants back to the water column. However, dispersion of contaminants discharged to the water from everyday shipping activity forms a significant knowledge gap with few exceptions (Hodgkins et al., 2019; Mestres et al., 2010; Ytreberg et al., 2020).

The aim of this paper is to analyze spatio-temporal dispersion of different contaminants in the marine environment directly released into the water along shipping lanes and in harbors. We use a state-of-the-art modelling system consisting of a framework made up of the Automatic Identification System (AIS) based Ship Traffic Emission Assessment Model (STEAM) (Jalkanen et al., 2009; Jalkanen et al., 2012; Johansson et al., 2013; Johansson et al., 2017; Jalkanen et al., 2021), the 3-dimensional General Estuarine Transport Model (GETM) (Burchard and Bolding, 2002; Bruggeman and Bolding, 2014) and the Eulerian tracer transport model.

Our hypothesis is that general circulation and vertical stratification of the region under consideration define the areas under the highest pressure by shipborne contaminants. These areas could be distant from shipping lanes and harbors.

We use basin-wide approach analyzing:

1) basin-wide pattern of shipborne contaminants released to the water with a daily resolution at the ship locations, either en-route or in the harbors;
2) basin-wide distribution patterns of dispersed contaminants on the surface, integrated over the water column and on surface sediments;
3) vertical spreading of the contaminants averaged over a selected area.

The target area of this study is the Baltic Sea, which is one of the busiest shipping activity regions in the world (Wu et al., 2017).

The Baltic Sea is a shallow (average depth of 54 m) semi-enclosed brackish European inland sea in the temperate climate zone. Its surface area is 422,000 km^2 and volume 21,205 km^3 (Leppäranta and Myrberg, 2009). Estuarine exchange due to freshwater runoff at the landward side of the sea and saline water inflows from the North Sea determines permanent stratification conditions. In general, vertical stratification in the Baltic Sea is characterized by a permanent halocline at a depth range of 60-80 m (Matthäus, 1984; Väli et al., 2013). A seasonal thermocline is present at a depth of 10-30 m in spring and summer. Thus, the upper mixed layer thickness varies from 10 to 30 m in spring and summer to 60-80 m in autumn and winter.

General circulation is cyclonic in the Baltic Sea (Meier, 2007; Jędrasik and Kowalewski, 2019), with the exception of the Gulf of Finland (Maljutenko and Raudsepp, 2019; Westerlund et al., 2019) and the Gulf of Riga (Soosaar et al., 2014; Lips et al., 2016). In these two basins, anticyclonic circulation is a significant feature during spring and

summer.

Seasonal sea ice coverage has an important effect on vertical stratification, general circulation and dispersion of any passive tracer introduced by anthropogenic activity. During the last decade, maximum ice extent has varied within a range of 30,000 km^2 (e.g. in 2015) to 260,000 km^2 (e.g. in 2011) (Uotila et al., 2015). In the ice season of 2019/20, only the coastal areas of northern Bothnian Bay were ice-covered (Raudsepp et al., 2021). The decrease in maximum ice extent and the length of the ice season, both of which have been observed in recent years (Raudsepp et al., 2020), may influence the spatial variation of vertical stratification of the Baltic Sea (Hordoir and Meier, 2012).

There are many marine protected areas (MPAs) in the Baltic Sea (Jonsson et al., 2020) where anthropogenic interference is undesirable. The Baltic Sea has only limited water exchange with the ocean through the Danish Straits, which results in a long residence time of the water and the contaminants of anthropogenic origin in the sea (Döös et al., 2004). The area is receiving contaminants from different sources suffering from the integrated impact of pollution. Even though the contaminant concentrations in individual discharges to the Baltic Sea often seem to be below the threshold levels of environmental quality standards, there is a suspicion that the cumulative effect may be permanently elevated and possibly in harmful concentrations (e.g. Endres et al., 2018; HELCOM, 2018).

2. Methods

2.1. The modelling system

The modelling system includes the ship emission model STEAM (Jalkanen et al., 2009; Jalkanen et al., 2012; Johansson et al., 2013; Johansson et al., 2017; Jalkanen et al., 2021) and the marine physical model GETM (Burchard and Bolding, 2002; Bruggeman and Bolding, 2014) together with the passive tracer model. The STEAM with AIS provides volume discharges of BW, GW, BA, BI, Food Waste (FW), SC, Stern Tube Oil (STO) and release of several compounds of AFP from ships to the water (Jalkanen et al., 2021). Combining the AIS data and the STEAM-based contaminant discharge, the gridded daily input of contaminants is applied as mass fluxes into the surface layer of the sea. The dispersion of contaminants is calculated using the GETM with a passive tracer model for the Baltic Sea.

Physical dispersion is described using three-dimensional Eulerian advection and diffusion equations for tracer concentration in mg/m^3. Each contaminant $C(t,x,y,z)$ can be expressed in the Cartesian x, y and z coordinate system as follows

$$\frac{\partial C(t,x,y,z)}{\partial t} = advection + diffusion + sedimentation + load$$

Advection term ($u\,\partial C/\partial x + v\,\partial C/\partial y + w\,\partial C/\partial z$) describes horizontal dispersion due to horizontal velocities u, v and vertical velocity w. Diffusion can be expressed as $[A_h\,(\partial^2 C/\partial x^2 + \partial^2 C/\partial y^2) + \partial/\partial z(\nu_z \partial C/\partial z)]$, where A_h and ν_z are horizontal and vertical diffusivities, respectively. Sedimentation is taken into account by means of settling velocity w_s as $(w_s\,\partial C/\partial z)$. The shipping load was implemented as the boundary condition at sea surface elevation ζ as $C(x, y, z{=}\zeta) = L(x,y)/dz(x, y, z{=}\zeta)$, where dz is layer thickness and $L(x,y)$ is the load from ships.

The model simulations were carried out for the year 2012, which can be considered as typical for hydrographic conditions relative to the climatological period 1993-2014 (von Schuckmann et al., 2018). Vessel activity data was collected for the whole Baltic Sea, including the Kattegat (Fig. 1), which is also the model domain for the GETM and passive tracer model. The model boundary was closed at Kattegat to avoid import of the contaminants from the North Sea. The GETM horizontal resolution was set to 1 nautical mile, and 40 sigma-coordinate adaptive layers (Gräwe et al., 2015) were used vertically. The coastline was adjusted according to shipping traffic to better resolve contaminant loads from harbor areas. Initial concentrations of the contaminants in the seawater were assumed to be zero. An hourly atmospheric forcing from the COSMO CLM version 5.0 (Geyer, 2014) was used. Tracer transport was updated at each baroclinic timestep of 500 s. Model output fields consist of daily average values.

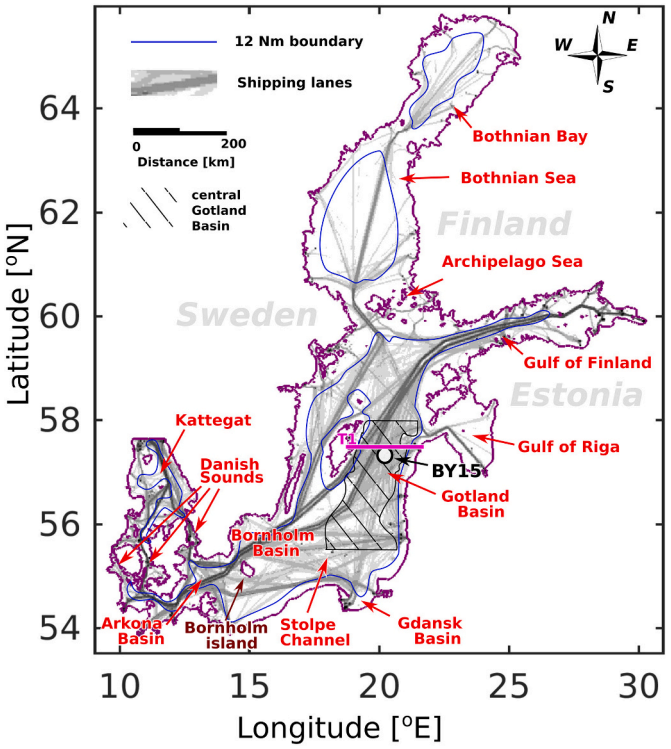

Fig. 1. The Baltic Sea domain and location of the Baltic Sea sub-basins and main shipping lanes. The blue line shows the border of a territorial water zone of 12 nautical miles from the coast. The transect T1 is shown with a pink line. The striped area in the central Baltic shows the area for spatial averaging. (For interpretation of the references to color in this figure legend, the reader is referred to the web version of this article.)

Detailed setups of the STEAM and GETM models for the year 2012 are provided by Jalkanen et al. (2021) and by Raudsepp et al. (2019), respectively. The GETM model has been validated for a long-term model hindcast of 1966-2006 (Maljutenko and Raudsepp, 2014, 2019) and for the year 2012 (Raudsepp et al., 2019).

2.2. Discharge of waste streams and leakage from antifouling paints

The AFP biocides leach continuously when the boats and ships are in contact with water (Fig. 2a). The load from AFP is dependent on the operating location of the ship, wet area of the hull and surface leaching rate of the particular chemical compound. Due to different regulations for AFP use in the Baltic Sea, there are different leaching rates defined for the Bothnian Sea, Baltic Proper and Kattegat area for each ship depending on its operation region. The calculation of leaching rates is described in detail by Jalkanen et al. (2021). We have used copper (Cu) leaching rates of 24.5, 15.5, 7.5 and 3.1 μg cm^{-2} day^{-1} for the ships operating internationally, in Kattegat, in the Baltic Proper (that is the common area for the Gulf of Finland, Gotland-, Bornholm- and Arkona Basins), and in the Gulf of Bothnia, respectively. The leaching rates for zinc (Zn) were set to 4.4, 4.6, 2.3 and 1.4 μg cm^{-2} day^{-1}, respectively. Due to seasonal ice cover in the Baltic, natural abrasion of sea ice reduces the antifouling paint use. Therefore, only 50% of ships operating in the Baltic Proper, including the Gulf of Finland and the Gulf of Riga, and 20% of ships in the Gulf of Bothnia are assumed to use AFPs.

Other sources involve the discharge of shipborne BI, SC, BW, GW, and BA water volume to the sea, which spatio-temporal occurrence is

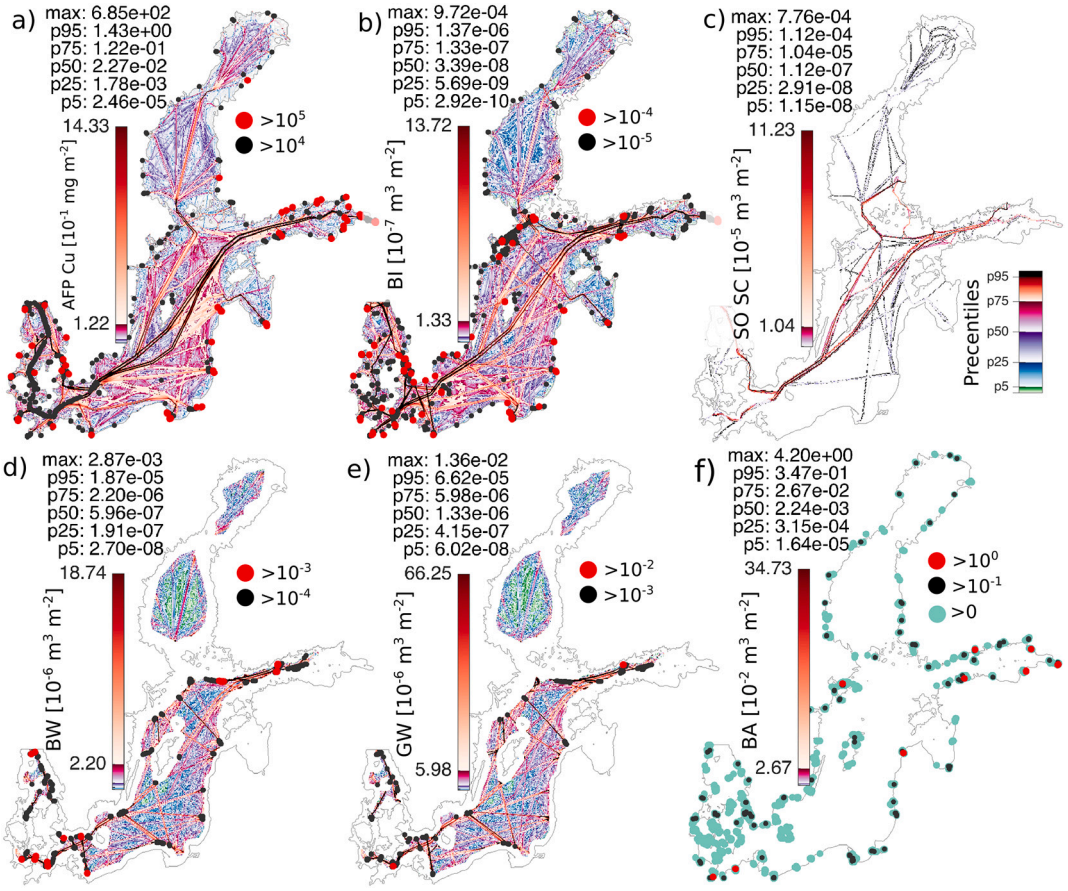

Fig. 2. The spatial distribution of annual discharge of copper from a) antifouling paint, b) bilge water, c) open- and closed-loop scrubber water, d) black water, e) grey water and f) ballast water. The color bars represent ranges of different percentiles (5, 25, 50, 75, 90). The values of the percentiles are shown at the color bars. The dots represent hotspots where the discharge exceeds the corresponding value. The maximum discharge of the corresponding waste stream is indicated in each subplot. Values of the discharges are calculated for each model grid cell of 1 × 1 nm.

controlled by the ship crew and should follow international and national regulations. The discharged water volume is determined by the STEAM model which takes into account the technical characteristics of the ships, the number of crew members and passengers as well as the discharge rules of various countries and IMO conventions (Jalkanen et al., 2021).

Onboard BI generation was assumed to depend on the vessels' main engine power in operation, and its release was modelled as a continuous flow from ships to the sea where allowed by law. There is no BI discharge in the Finnish Archipelago Sea as no ships enter this area due to its shallowness and numerous islands (Fig. 2b). In addition, we have to keep in mind that a Finnish national legislation prohibits discharge of BI closer than 4 nautical miles from the shore.

In 2012, only five vessels were identified with existing scrubber installations. Therefore, the 2012 scrubber discharge pattern consists of only a few lines (Fig. 2c), but the annual SC discharge volume of $1.54*10^6$ m^3 is comparable to the discharge volumes from the other sources. In recent years, the number of ships equipped with scrubbers has increased up to 4000 units (DNV-GL, 2020; Jonson et al., 2019) and the corresponding load pattern is presented by Jalkanen et al. (2021).

The discharge volumes of BW and GW depend on the number of people on board ships, time spent on board, discharge rate and the speed of a vessel. The coastal areas are free from discharges of BW and GW due to international regulations which prohibit discharges of BW and GW closer than 12 nm from the shore (Fig. 2d, e). The BW and GW are accumulated in the tanks of the ships within the prohibited areas and are discharged in large amounts once the ships have left the 12 nm zone. In general, the discharge volumes of GW are an order of magnitude larger than the volumes of BW (Fig. 2d, e).

The volume of BA discharge is governed by vessel size, type, number of port calls and the factor which describes the portion of BA compared to the BA capacity. Since BA discharge takes place only near the harbors, the spatial discharge pattern consists of point sources (Fig. 2f).

2.3. Loads of the contaminants

Over 600 contaminants discharged to the sea from the ships were identified. This is a large number and it is not possible to include all of them in the simulations. We selected five contaminants representing different sources and chemical classes: Cu, Zn, naphthalene (Nap), pyrene (Pyr), and dibromochloromethane (DBCM). Cu and Zn are mainly leached from AFP. The loads of Cu and Zn from SC, BI, GW and BW are several orders of magnitude lower (Table 1). Nap is emitted in high amounts from BI but is also present in GW and BW. Open loop scrubbers (SO) are the main source of Pyr, but they are contributed by BI and GW (Table 1). DBCM is emitted from BA in a very high amount (Table 1). Preliminary assessment of BA concentrations and toxicity data show that the ratio between predicted environmental concentrations and predicted no effect concentration (PEC/PNEC) of DBCM is >1, which indicates a risk for harmful effects on the environment (Delacroix et al., 2013). The selection of Nap and Pyr is also relevant since these compounds have different degradation rates in the environment (Guha et al., 1999).

The spatial distribution of loads $L_c(x,y)$ for each contaminant is calculated based on hourly discharges of wastewater $V_i(x, y)$ and antifouling paint emission $L_{c,\ AFP}(x,y)$ from the STEAM model as follows:

Table 1
The loads and concentrations of contaminants from different shipping waste streams. Each volumetric emission (BI, GW, BW, SO, SC and BA) is complemented with concentration (mg/m^3) and total annual load to the Baltic Sea (t). Last two columns show the used adjustment factor a_c and total annual load of the contaminant from all emissions.

	Leaching	Emissions													
	AFP	BI		GW		BW		SO		SC		BA			
Emission [m^3]	–	3.2*10^5		5.5*10^6		1.38*10^6		1.53*10^6		1.09*10^4		4.08*10^8			
Contaminant	Load	Conc	Load	Conc	Load	Conc	Load	Conc	Load	Conc	Load	Conc	Load	a_c	Total
Cu	299.3	126	0.041	289	1.6	312	0.43	116	0.18	587	0.0064	–	–	0.97	292.5
Zn	59.3	568	0.18	628	3.5	400	0.55	173	0.26	298	0.0033	–	–	0.9	57.4
Nap	–	49.6	0.016	0.0420	0.00023	1.97	0.0027	–	–	–	–	–	–	0.80	0.015
Pyr	–	1.46	0.00047	0.0300	0.00017	–	–	1.58	0.0024	–	–	–	–	0.80	0.0024
DBCM	–	–	–	3.25	0.018	27.7	0.038	–	–	–	–	21.6	8.79	0.93	8.23

$$L_c(x,y) = a_c \left(L_{c,AFP}(x,y) + \left(\sum c_i \, V_i(x,y) \right) \right),$$

where a_c is an adjustment factor for each contaminant and c_i is the concentration of contaminant in an i-th type of discharge (Table 1). The multiplier a_c is an adjustment factor for removing a fraction of the load which is assumed to leave the system due to various marine processes. A fraction of 3% of Cu and 10% of Zn is assumed to be adsorbed to detritus and suspended particulate matter (van Hattum et al., 2016) and settling in the water with a sedimentation velocity of 4 m/day. We choose the value of 4 m/day based on the sinking velocity measurements of different phytoplankton cells and aggregate material (Bach et al., 2012). Resuspension is suppressed to accumulate Cu and Zn particles into sediments. The sedimenting fraction of Pyr of 20% was not simulated. Instead, it was removed from the load. According to our expert knowledge, we have estimated that 20% of Nap load is removed from the system to mimic biodegradation. An evaporation fraction of DBCM of 7% was removed directly from load (Fisher et al., 2014; He et al., 2019).

Background loads from rivers and atmosphere were neglected for a clear shipping signal and due to scarce data of corresponding loads. Additionally, no-flux boundary conditions were used at the Kattegat (Fig. 1).

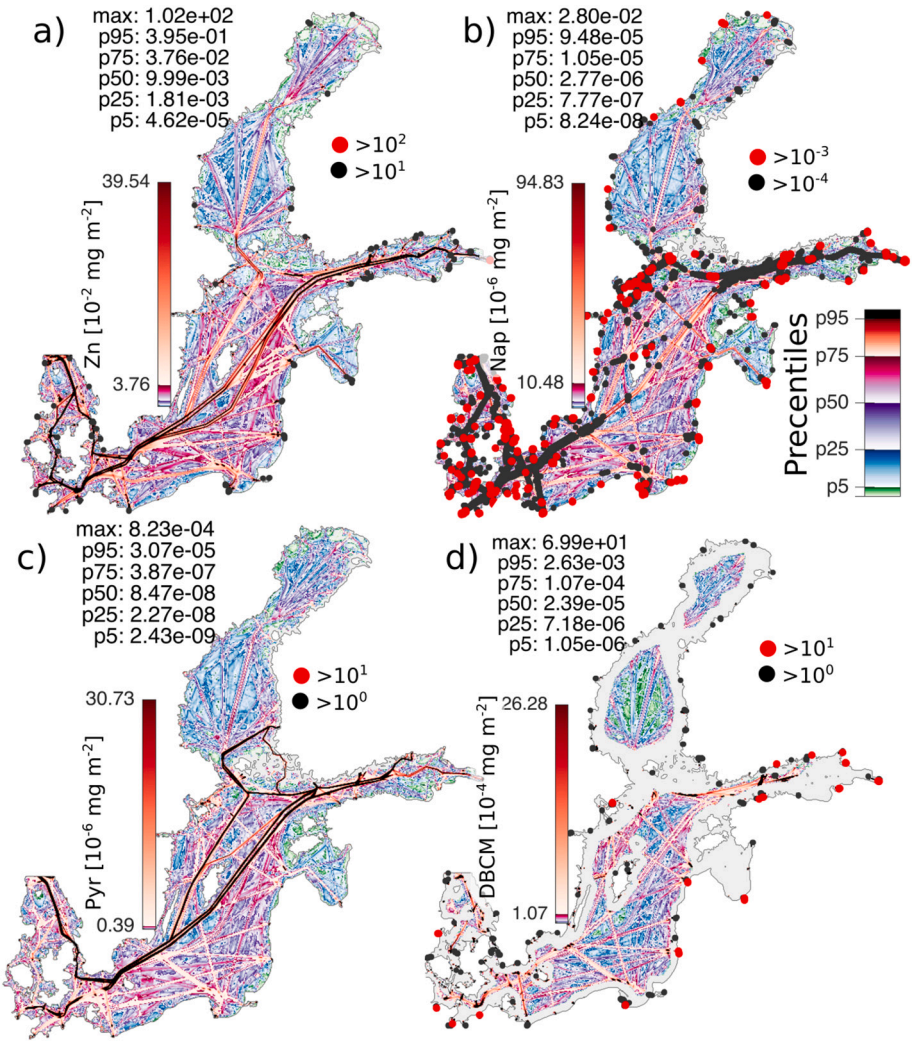

Fig. 3. The spatial distribution of the annual emission of a) zinc, b) naphthalene, c) pyrene and d) dibromochloromethane. The color bars represent ranges of different percentiles (5, 25, 50, 75, 90) of the annual emission of the contaminants. The values of the percentiles are shown at the color bars. The dots represent hotspots where the load exceeds the corresponding value. Maximum load of the corresponding contaminant is indicated in each subplot. Values of the loads are calculated for each model grid cell of 1 × 1 nautical mile.

3. Results

3.1. Loads of the contaminants

The spatial distributions of annual loads of selected contaminants originating from different sources are shown in Fig. 2a for Cu and on Fig. 3 for other contaminants. AFP contributes 99% to the total Cu load and 93% to the total Zn load (Table 2). The loads of Cu and Zn have a similar pattern (Figs. 2a, 3a), but annual loads of Zn are about an order of magnitude lower (Table 2). In the Baltic, the annual input of Cu of 290 t from shipping constitutes 2% of the global Cu load from AFP (Blossom, 2002) and 30% of the overall waterborne (rivers, coastal areas and unmonitored rivers) input of Cu into the Baltic Sea (886 t). This is a considerable amount, comparable to the entire riverine Cu input into the entire Gulf of Finland (290 t) (HELCOM, 2011). The input of Zn from shipping (60 t) is of less importance, constituting ca. 2% of the background input from waterborne sources (rivers, coastal areas and unmonitored rivers) to the Baltic Sea (3157 t). Shipping related input of Zn into the marine waters is comparable to the total riverine Zn input of Estonia (HELCOM, 2011).

Majority of Nap (84% of total load) is emitted from BI (Table 2), and therefore the characteristic pattern of Nap resembles general shipping activity with hotspots close to the largest harbor areas, where loads exceed 10^{-3} mg/m^2 per year (Fig. 3b). The loads in excess of 10^{-4} mg/m^2 are distributed across medium and small harbors and in the Stockholm Archipelago, on the shipping lines in the Gulf of Finland, southern Baltic Sea, Danish Sounds and Kattegat. The release of Nap has a 14% share in the BW emission, which contributes to the load in above-mentioned areas due to intense passenger ship traffic.

A Pyr load of 80% is related to SO discharges (Fig. 3c, Fig. 2c). However, a small fraction of Pyr contamination is distributed across the Baltic Sea due to its content in BI streams. The most distinct distribution characteristic of Pyr is the absence of hotspots.

DBCM distribution integrates the load from BA and contribution from the BW and GW discharges. Due to DBCM abundance in BA, there are many hotspots in large harbors (Fig. 3d). Outside the 12 nm coastal zone, DBCM load is related to passenger traffic. The narrow regions in the Gulf of Finland and in the Danish Sounds have the largest offshore loads. Total load of DBCM is much larger than Nap and Pyr loads.

3.2. Dispersion of the contaminants

We have considered the case where ship-discharged contaminants enter an otherwise “pristine” marine environment. To describe temporal evolution of the pollution we have extracted surface concentrations of the contaminants along the transect T1 and areal mean concentration profiles in the central Baltic proper (see Fig. 1). The transect extends from the source-free coast across the main shipping lane to the hotspot at the opposite coast. The vertical distribution of areal mean concentration of the contaminants has been evaluated for the open sea in the Gotland Basin (Fig. 5a). We have excluded harbors because the contaminant concentration is an order of magnitude higher there than in the open sea and will prevail when horizontal integration has been performed.

The period from January to June can be characterized as a spin-up of the contaminant fields in the open Baltic Sea (Figs. 4, 5). The concentration increases monotonically in the open sea, which is well illustrated in the vertical distribution of the contaminants (Fig. 5). The water column is mixed down to the pycnocline at about 70-80 m (Fig. 5b). Similarly, the contaminants are rapidly mixed to that depth, leaving no high concentration trace at the surface (Fig. 4). The shipping lanes do not emerge in the overall concentration field, except in the case of Pyr (Fig. 4e) which is discharged along the main shipping lane in high quantities (Fig. 3c). There is a continuous discharge of Cu, Zn, Nap and DBCM (see Fig. 5 for the load in the Gotland Basin) in the shipping lines, but Pyr has a discrete event-type load when ships with scrubbers cross the Baltic Sea (Fig. 5). In that respect, surface distribution of Pyr concentration characterizes horizontal dispersion of the discharged contaminants from the shipping lanes best (Fig. 4). Therein, the dispersion distance across the shipping lane is about 60 km. Clearly elevated concentrations of the contaminants could be visible in the range of 10 km for a few days only. A high concentration of contaminants at the hotspots stands out in overall surface concentration fields (Fig. 4), which is well illustrated in the distribution of DBCM (Fig. 4f). The DBCM is discharged in large amounts at the harbors as the marker for the BA waste stream (Fig. 3f).

The second period represents the basin-wide spreading of shipborne contaminants. The discharges to the ship lanes are hardly distinguishable (Fig. 4). Physically, it is explained by a combination of two significant processes: 1) the increase of the kinetic energy of the surface layer currents (Fig. 4a) and 2) the development of a seasonal pycnocline that restrains downward vertical mixing of the contaminants (Fig. 5b). More specifically, the seasonal thermocline starts to develop in the upper layer in May due to surface warming. At the base of the thermocline, the vertical gradient of the contaminants increases continuously due to a continuous load of contaminants at the surface (Fig. 5). The peak of surface concentration of contaminants, except Nap, is seen in August-September (Fig. 5), although the seasonal thermocline begins to erode from September due to surface cooling of the sea and an increase of wind-induced mixing. The contaminants become mixed deeper, which is manifested by the increase of the depth of the high gradient layer (Fig. 5). Also, their surface concentration decreases despite of the continuous load. Horizontal spreading of the contaminants is limited in distance (Fig. 4) as they are more readily mixed into the subsurface layer. Still, each passing of a ship with SC discharge leaves a distinguishable trail of higher Pyr concentration, compared to the surrounding water, for a few days (Fig. 4e). By the end of the year, the contaminants have reached a depth of about 140 m, but in small concentrations (Fig. 5).

Seasonal development of one-year surface concentration fields of the contaminants is shown on Fig. A1. By the end of the one-year simulation, no distinguishable shipping lanes with high concentrations of discharged chemicals can be detected on the surface (Fig. 6). The contaminants are widely spread over the Baltic Sea, but half of the area has low surface concentrations of contaminants (50 percentile). The harbors with a significantly higher load of Cu, Zn, Nap and DBCM are still distinguishable (Fig. 6a–c, e). Sub-regionally, the Gulf of Finland and Kattegat/southwestern Baltic Sea emerge as areas of the highest concentration of surface contaminants, which correspond to the highest load due to a convergence of shipping lanes and the presence of a high number of hotspots. All contaminants show a similar surface distribution

Table 2
The share of contaminants in AFP leaching and different shipping waste streams.

	Shipping emissions							
Contaminants	AF Cu	AF Zn	BI	BW	GW	BA	SO	SC
Copper	99.26%		0.01%	0.14%	0.53%		0.06%	<0.01%
Zinc		93.01%	0.29%	0.86%	5.42%		0.41%	0.01%
Naphthalene			84.41%	14.37%	1.22%			
Pyrene			15.35%		5.41%		79.23%	
Dibromochlorometahne				0.43%	0.20%	99.37%		

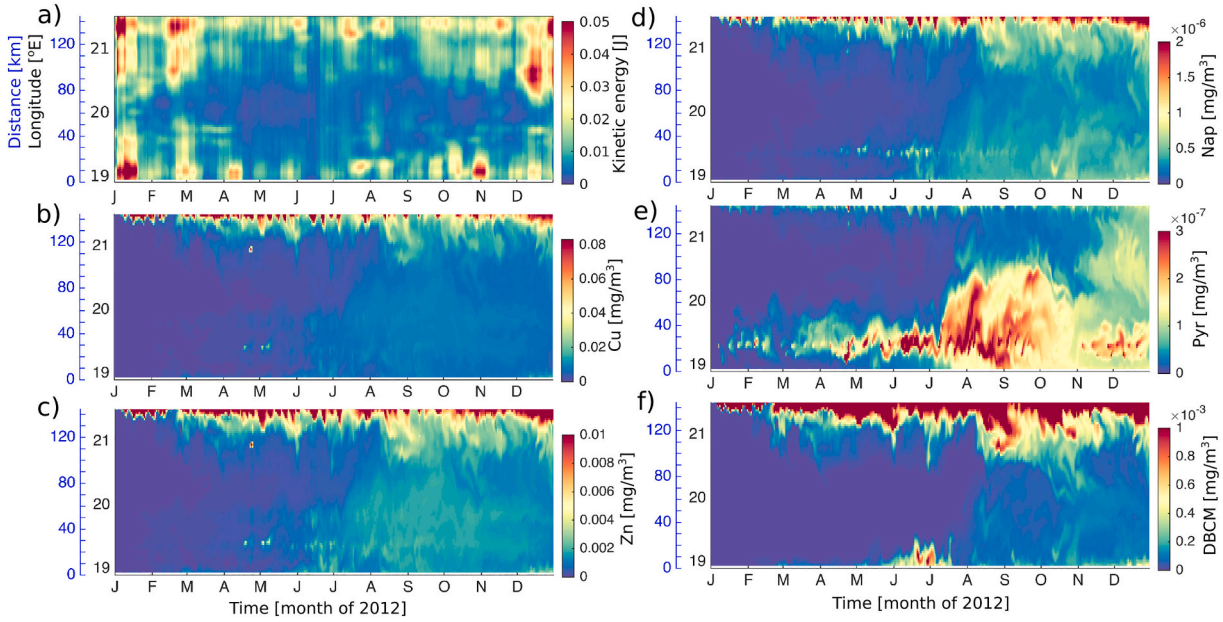

Fig. 4. Temporal evolution of spatial distribution of kinetic energy $(u^2 + v^2)^{½}$ of the surface currents (a), the surface concentration of copper (b), zinc (c), naphthalene (d), pyrene (e) and dibromochloromethane (f) along transect T1 shown on Fig. 1. Temporal evolution of spatial concentration distribution along X transect shown on Fig. 1. The blue axis, on the left, shows distance in km from the western shore of the eastern Gotland basin and the black axis shows the corresponding longitudes. (For interpretation of the references to color in this figure legend, the reader is referred to the web version of this article.)

pattern for concentrations above 75 percentile. This is well illustrated in the plots of surface distribution of standardized concentration of each contaminant. A high concentration of the contaminants over the northern and eastern Gulf of Finland corresponds to the mean northward currents there in December (Fig. 6f). We have to note that this current pattern, which was present for about a month, only changed in the last days of December. Relatively high concentrations of the contaminants at the southeastern Finnish coast of the Bothnian Sea indicate the transport pathway of the contaminants from the Gulf of Finland to the Bothnian Sea.

The surface distribution of the contaminants represents short time scale dispersion of recent load but says nothing about the contaminants distributed in the subsurface layer. Therefore, the concentration of the contaminants was integrated vertically over the upper 80 m deep layer, which corresponds to the mass of the respective contaminant per square meter. The layer thickness of 80 m was selected because the upper boundary of the permanent pycnocline corresponds to the depth of 80 m in the Baltic Sea (Fig. 5b). Additionally, a major part of the annual load of the contaminants remains in that layer, as can be judged from the vertical distribution (Fig. 5). Thus, here is presented spatial distribution of the mass of contaminants at the end of the first year simulation (Fig. 7). The pollutant mass at the hotspots is about an order of magnitude lower than the maximum annual load values there (Figs. 3, 7).

The Gulf of Finland, Kattegat and the southwestern Baltic Sea have the highest mass of contaminants, while the Gulf of Bothnia has the lowest, which is consistent with the geographical distribution of the loads. The south-eastern Bothnian Sea is affected by the transport of the pollutants from the western Gulf of Finland and northern Baltic Proper (Fig. 7f). A relatively high mass of the pollutants over the southwestern Baltic Sea, Arkona and Bornholm Basins, Stolpe channel and the Gdansk Basin corresponds to the general water transport from the Kattegat downstream in the cascade of the Baltic Sea subbasins (Fig. 7f). Pyr mass distribution (Fig. 7d), the load of which has high values over the offshore area of the Baltic Sea, best reflects the transport pattern. The stripe of elevated mass of the contaminants in the northern Baltic Proper and Western Gotland Basin is the result of the load along the major ship lanes there but also the transport from the Gulf of Finland and the cyclonic circulation pattern over the northern Baltic Proper (Fig. 7f).

Major shipping lanes and Cu and Zn loads in the harbors are well represented in bottom sediment distribution (Fig. 8). The highest masses per square meter are in Kattegat, southwestern Baltic Sea and in the Gulf of Finland. Compared to the width of shipping lanes, the sediment affected area is wider due to advective transport in the water column when Cu and Zn particles are settling. For example, for each 100 m of water column thickness, the Cu and Zn particles settle for 25 days with a prescribed settling velocity of 4 m/day. In narrow straits, like the Danish Sounds, the cross-shiplane advection is suppressed and the stripe of high concentrations of Cu and Zn in the sediments is narrow.

4. Discussion

In this study, a state-of-the-art method is used to model the shipborne waste streams and leakage of antifouling paints that contribute to the pollution of the marine environment. Simulation of the dispersion of the contaminants during a year, using a general circulation model, aims to partly fill in a significant gap that exists between the knowledge of the contaminants discharged from ships and their fate in the marine environment. One of the main steps forward was the use of a basin-scale approach, i.e. not limiting the study to a particular area, a ship, a single source or contaminant. Using the STEAM model and AIS data in combination enables us to move from the approach of artificial discharge patterns to operational discharges of shipping-related pollution (e.g. Magnusson et al., 2018; Ytreberg et al., 2020).

A fully three-dimensional ocean circulation model enables detailed studies describing the complete dispersion pattern of the discharged contaminants over time. The surface distribution of the contaminants depends on the spatial distribution of the sources, kinetic energy of the currents at the location of the discharges, vertical mixing and persistency of the surface circulation pattern. Depending on the penetration depth of surface-induced vertical mixing, i.e. vertical stratification, a vertically integrated current pattern is more relevant for explaining the spatial distribution of the contaminants than solely surface currents. At the coastal region, upwelling/downwelling events are associated with high vertical velocities forcing vertical transport of the contaminants. In the open sea area, vertical advection velocities are relatively small

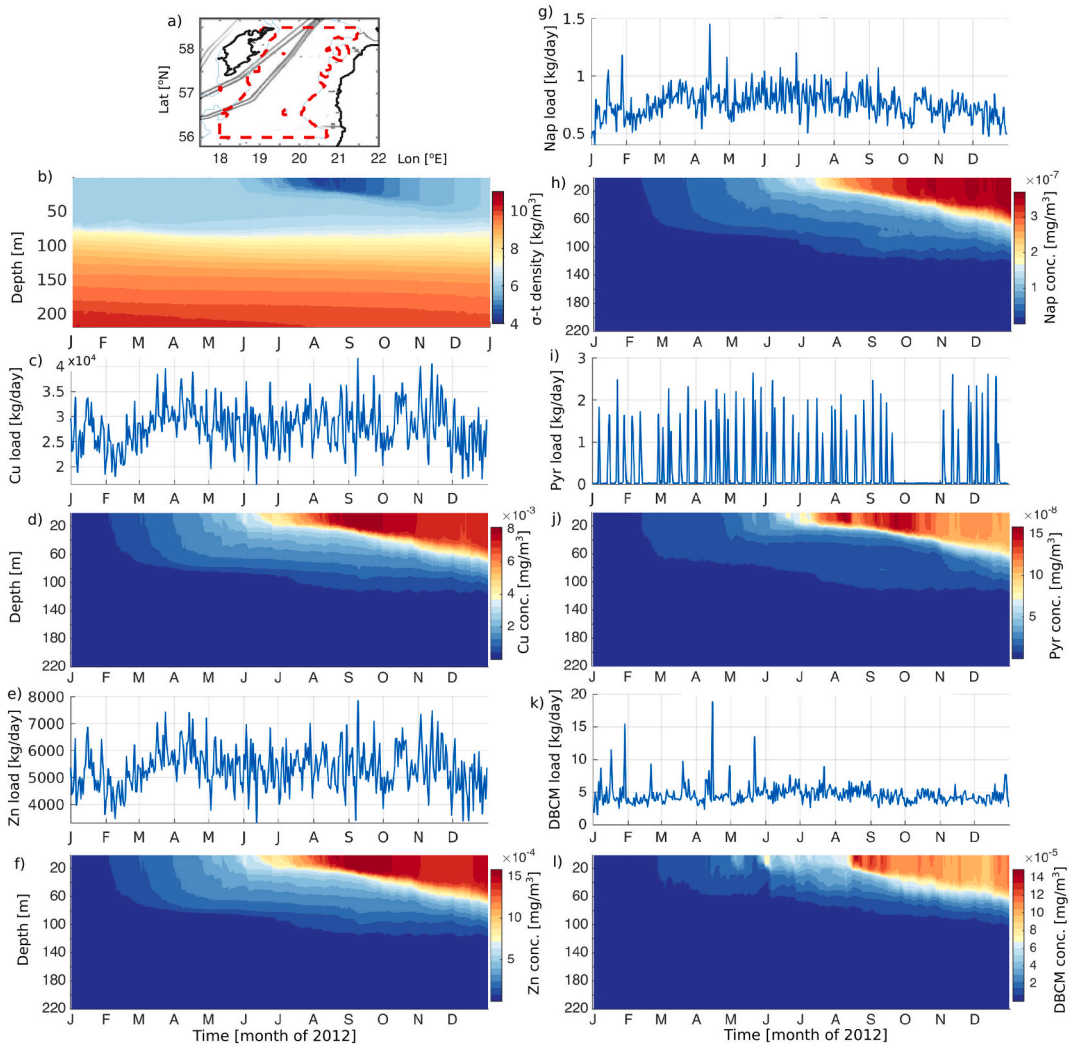

Fig. 5. The area of central Gotland Basin on a) and time-depth plot of corresponding area mean density on b). The time series of integrated load and time-depth plots of horizontally averaged concentrations are shown on c) and d) for copper, e) and f) zinc, g) and h) for naphthalene, i) and j) for pyrene, and k) and l) for dibromochloromethane. The region over which loads have been integrated, and the contaminants have been averaged is shown with a dashed red color line on a) and on Fig. 1. (For interpretation of the references to color in this figure legend, the reader is referred to the web version of this article.)

compared to the temporal course of vertical mixing. Although surface concentrations of the contaminants remain persistently higher than in the water column (Fig. 4), the vertically integrated mass/amount of the contaminants potentially has a stronger impact on living organisms, as they are spread over the water column. The surface currents that are responsible for the initial dispersion of the contaminants discharged from the ship are variable in time. Therefore, estimation of impacted areas using surface water circulation depends on the persistence of the circulation pattern, which can vary over the time scale from hours to a month.

Spatial distribution of the mass of the contaminants in the water column is the result of vertically integrated transport. In the Baltic Sea, general circulation is cyclonic (Meier, 2007), which results in transport of the contaminants from the heavily polluted southwestern Baltic Sea to the Gulf of Gdansk. The heavy load on the shipping lanes in the Eastern Gotland Basin is transported towards the eastern coast of the Baltic Sea and northward thereafter. In the Gulf of Finland, strong coastal offshore water exchange at the southern coast (Maljutenko and Raudsepp, 2019) results in transport contaminants discharged at the main harbors of the southern coast (Paldiski, Tallinn and Muuga harbors) to be transported to the central Gulf. The southeastern Gulf of Bothnia is under the pressure of shipborne contaminants discharged in the western Gulf of Finland and passenger ships that operate between Helsinki and Stockholm. Thus, vertically integrated transport explains the spreading of the contaminants from the high discharge area elsewhere.

In this study, we have excluded all other sources of contaminants besides shipping. In addition to direct input from shipping, atmospheric deposition both from shipping and land-based sources are one of the major sources for contaminants in the open sea. Quantitative estimation of atmospheric deposition of different contaminants emitted by ships requires a separate study. Although Hermansson et al. (2021) have provided emission factors for different chemicals from ships, the atmospheric transport and chemistry model is needed for the calculation of the fate of the chemicals in the atmosphere and their deposition to the sea. Therefore, we compare the annual load of the contaminants discharged to the Baltic Sea from this study and the rough estimates of total atmospheric deposition of the same contaminants. According to Settimo et al. (2021), the estimates of atmospheric deposition rate for Cu, Zn, Pyr and Nap are about 0.8 μg/(m^2d^1), 5 μg/(m^2d^1), 10 ng/(m^2d^1) and 100 ng/(m^2d^1), respectively. For the whole Baltic Sea (area of 377,000 km^2), the annual atmospheric load would be about 100 tons of Cu, 700 tons of Zn, 1 ton of Pyr and 10 tons of Nap. Thus, annual atmospheric loads of Pyr and Nap are three orders of magnitude higher than the loads from ship discharges, an order of magnitude higher for Zn and several times

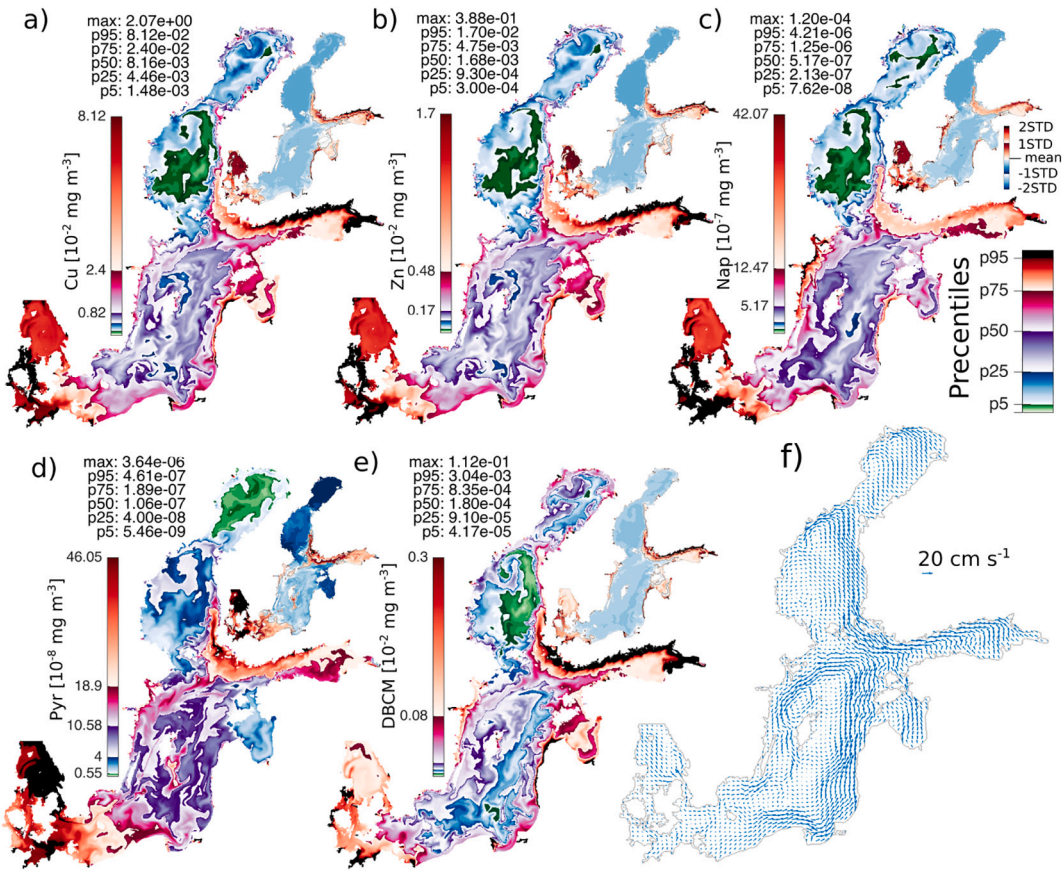

Fig. 6. The concentrations of a) copper, b) zinc, c) naphthalene, d) pyrene and e) dibromochloromethane at the surface on 31 December 2012. Different color shades of green, blue, violet, pink and red show the ranges of 5th, 25th, 50th, 75th and 95th percentiles of the concentrations, respectively. The values of percentiles are shown in each subplot. The insets show standardized concentrations of each contaminant calculated as $(C(x,y) - \mu_C)/\sigma_C$, where μ_C and σ_C are spatial average and standard deviation of the concentration distribution $C(x,y)$ on 31 December 2012. The surface layer currents averaged over December f). (For interpretation of the references to color in this figure legend, the reader is referred to the web version of this article.)

lower for Cu (Table 2). Liu et al. (2020) have shown that there is net oceanic DBCM emission over the western Pacific Ocean and the East China Sea. The other sources are either located at the coast, like rivers and streams, or within the coastal zone, like wastewater and production water outlets. These sources represent point sources, while an entire coastline could be considered as a diffusive source from where the pollutants can leach into the marine environment. Thus, we have provided the spatial distribution of the concentrations of the contaminants discharged from shipping to the pristine sea. At present stage, we have not considered physicochemical and biological processes that decrease the concentration of the contaminants in the water. Comparison of simulated concentrations and measured background concentrations enables insight into the share of annual shipborne pollution in the overall pollution of the sea. For the following comparison, we have used a 95-percentile value for the surface concentration of contaminants (Fig. 6).

Our modelled Cu and Zn concentrations (Fig. 6) are about an order of magnitude lower than the background concentrations of the Baltic Sea of 0.5-0.7 mg/m^3 for Cu (Kremling and Streu, 2000; Pohl and Hennings, 2005) and 0.6-1 mg/m^3 for Zn (Kremling and Streu, 2000; Pohl and Hennings, 2005). When we extend the model simulation to 5-years by repeating one year simulation five times (e.g. Raudsepp et al., 2019), then the concentration of Cu becomes comparable to the background values (Fig. A2). Natural concentrations of Cu are typically between 0.03 and 0.25 mg/m^3 (e.g. Bowen, 1985; Kremling and Pohl, 1989) and Zn of 0.005-0.3 mg/m^3 (Kremling and Streu, 2001) for surface seawater of the Northern Atlantic.

We have used Nap as a marker contaminant for the BI and Pyr for the SC. The data about Nap and Pyr concentrations in seawater are scarce compared to the data on the Baltic Sea sediments, mussels and fish (Baumard et al., 1999; Lubecki et al., 2006; Robinson et al., 2017), which shows that these contaminants potentially accumulate in biota. Still, measured Nap and Pyr concentrations in the Baltic Sea vary between (0.05-1.8)*10^{-3} mg/m^3 and (0.025-1.0)*10^{-3} mg/m^3, respectively (Witt, 1995), which are several orders of magnitude higher values than the values due to shipping in our model simulation. By the end of the fifth-year simulation the surface concentrations of Pyr have increased up to five times compared to the one-year simulation (Fig. A2).

Considering the increased number of scrubbers installed on ships that operate in the Baltic Sea (Jonson et al., 2019), the SC discharge volumes have been increased by almost two orders of magnitude compared to the discharge in the present study (Jalkanen et al., 2021). This involves also an increased load of all contaminants that have been identified in the scrubber discharge water. We have used Pyr as a marker for the SC, but in addition, significant concentrations of different metals have been measured in scrubber effluent (Koski et al., 2017; Hassellöv et al., 2020).

DBCM concentrations have been measured in the range of 0.03-15*10^{-3} mg/m^3 in the Atlantic Ocean (Schall et al., 1997; Bravo-Linares et al., 2007) and in the coastal waters at different sites (Liu et al., 2011; He et al., 2019). A few measurements performed in the Gdansk Bay of the Baltic Sea show DBCM concentrations up to about 0.05 mg/m^3 (Biziuk, 2001). These measurements have been performed at the coasts of the Gdansk Bay, which is surrounded by densely spaced industry and many harbors. In comparison, in the mesocosm experiments of the Baltic Sea water, DBCM concentrations of about 0.6*10^{-3} mg/m^3 were

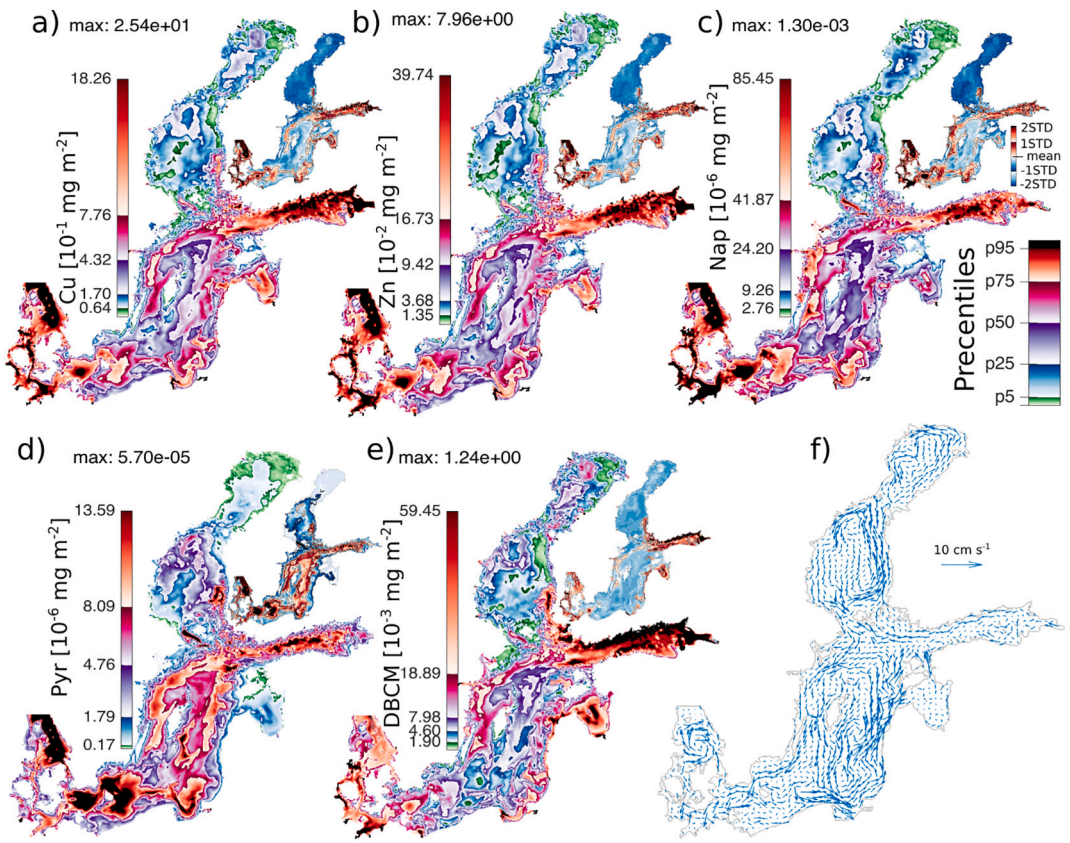

Fig. 7. The mass per area of a) copper, b) zinc, c) naphthalene, d) pyrene, and e) dibromochloromethane integrated over an 80 m deep surface layer on 31 December 2012. Different shades of green, blue, violet, pink and red show the ranges of 5th, 25th, 50th, 75th and 95th percentiles of the mass per area, respectively. The values of percentiles are shown in each subplot. The insets show standardized mass per area of each contaminant calculated as $(D(x,y) - \mu_D)/\sigma_D$, where μ_D and σ_D are spatial average and standard deviation of the mass per area distribution $D(x,y)$ on 31 December 2012. The mean currents over an 80 m deep surface layer are averaged over the year 2012 (f). (For interpretation of the references to color in this figure legend, the reader is referred to the web version of this article.)

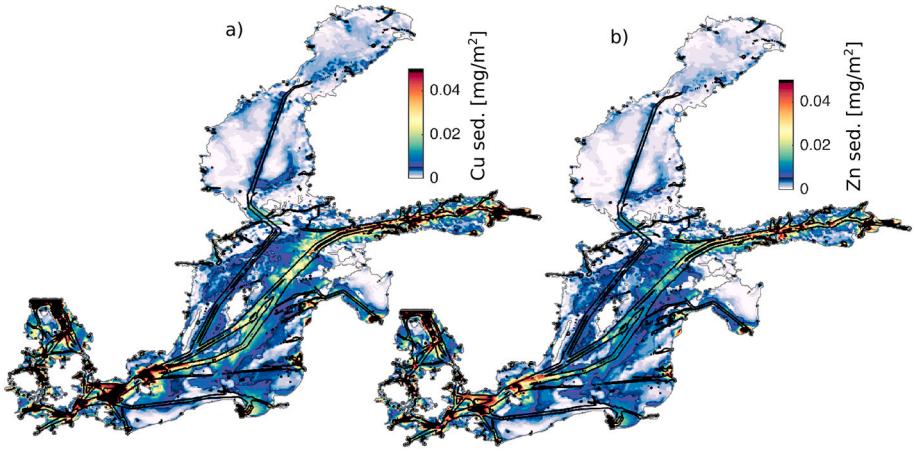

Fig. 8. The horizontal distributions of a) copper and b) zinc on the seafloor at the end of the year 2012. The main shipping lanes are shown as black lines.

measured (Webb et al., 2016). The contribution of DBCM by shipping according to our model results are comparable to the reported concentrations.

The modelled environmental concentrations in the water were compared with environmental quality standards (EQS). For Cu and Zn, EQS values of 1.45 and 1.1 mg/m^3 were derived from the Swedish Agency for Marine and Water Management (HVMFS, 2013:19). For DBCM, an EQS value of 6.3 mg/m^3 was obtained from the IMO GESAMP Ballast Water Working Group (GESAMP, 2019). EQS value for naphthalene (1.2 mg/m^3) was obtained from (EU Directive 2008/105/EC) and EQS for pyrene (0.023 mg/m^3) was obtained from RIVM (2012). Compared to simulated surface concentrations, exceedance of EQS for Cu (Fig. 6) could be expected in a specific location and for a limited time. At highly Cu polluted areas, the measured average concentrations of Cu have varied from 2 to 4 mg/m^3 at different sites of the Neva Estuary (Gubelit et al., 2016) and from 1.5 to 16.7 mg/m^3 in the Gulf of Gdansk (Zaborska et al., 2019). The Zn concentrations in seawaters of the Gulf of Gdańsk ranged from 0.1 to 4 mg/m^3 in the last decade (Zaborska et al.,

2019). Our results show a Cu concentration as high as 1 mg/m^3 in the Neva Estuary, which is relatively close to the EQS value, and 0.01-0.23 mg/m^3 in the Gulf of Gdansk. Elevated concentrations of Cu (5-10 mg/m^3) and Zn (10–40 mg/m^3) have been measured in marinas (Hall and Anderson, 1999; Matthiessen et al., 1999; Boxall et al., 2000; Munari and Mistri, 2007), which are high due to AFP leaching from leisure boats (Ytreberg et al., 2010). In this study we have not taken into account Cu and Zn release from leisure boats, which have been estimated at 57 t for Cu and 49 t for Zn annually (Johansson et al., 2020). Leisure boats contribute to Cu and Zn pollution mainly along the coastline and during summer when coastal sea ecosystems are most vulnerable. Thus, there could be areas in the Baltic Sea where shipborne contribution of Cu and Zn may lead to concentrations that exceed EQS for an elongated period of time or even permanently.

The other pressure of shipborne pollution is to the biota in Marine Protected Areas (MPA). The MPAs are located mainly in the coastal sea (see Fig. 1 by Johansson et al. (2020) for the location of the MPAs) and are not critically affected by ship traffic unless large harbors are located in the neighborhood. We would like to point out two MPAs, southeastern Gulf of Bothnia and the southern coast of the Baltic Sea, that are not affected by direct input from shipping, but could be under pressure due to dispersion of shipborne contaminants. Comparison of the maps of the concentrations of the contaminants (Fig. 7) and MPAs in the Baltic (Fig. 1 by Jonsson et al., 2020) shows that MPAs in the northern Gulf of Finland and the Danish Sounds could be under the heaviest pressure from shipping discharges.

We have modelled five out of several hundred contaminants, but included all major waste streams from the ships. Water circulation resulted in a relatively similar spatial distribution pattern of the contaminants despite the varying spatio-temporal distribution of the discharge from waste streams. Therefore, we suggest that pollution pressure from shipping is far larger than that of the five contaminants considered in this study.

5. Conclusions

Heavy discharge takes place in the harbors and shipping lanes with high shipping intensity. These marine areas are under immediate pressure from the pollutants released by ships. In the Baltic Sea, these main areas are the Danish Sounds, the southwestern Baltic Sea and the Gulf of Finland. The initial dispersion of the contaminants is controlled by surface currents and vertical stratification. Higher surface kinetic energy and weaker stratification results in rapid dispersion of the contaminants from the ship lanes and vice versa. In the Baltic Sea, the dispersion of the contaminants is more intensive from autumn to spring than in summer. In summer, the surface concentration of the contaminants is higher, which implies heavier pressure to the seasonal marine organisms that inhabit the sea surface.

By the end of one-year simulation, shipborne contaminants are dispersed over the Baltic Sea by annual mean horizontal transport. Thus, the main circulation scheme of a particular water basin points out the sea areas that could be under significant pressure of operational shipborne pollution. Flow convergence zones could be potential accumulation areas of the contaminants.

We have modelled the dispersion of five contaminants out of several hundred that were detected in the waste streams. Annual load was in the order of 100 s of tons for Cu, 10s of tons for Zn, tons for DBCM, 10s of kilograms for Nap and kilograms for Pyr. Scrubber wash water release has increased from 1.5 mil m^3 in 2012 to 76 mil m^3 in 2018 (Jalkanen et al., 2021), which has also resulted in a Pyr load of 100 s of kg and an increase of Cu and Zn load of 10s of tons (Table 1). Although, for the vast area of the Baltic Sea, shipborne Cu and Zn concentrations remain much lower than background concentrations after one-year simulation. Maximum concentrations, especially Cu concentrations, may exceed the corresponding EQS values locally.

The results are based on ship traffic data for the year 2012, which consist of the corresponding discharges of wastewater and the loads of contaminants, and influenced by atmospheric and marine conditions present in 2012. The intensity of ship traffic varies annually and the same holds true for atmospheric and marine conditions, which influence the actual discharge of contaminants and their spreading in the sea. Main ship routes do not change from year to year, and hence, the general pattern of contaminant discharge from ships is fairly constant. The vertically averaged flow pattern in 2012 demonstrates the main features of the general water circulation in the Baltic Sea, which means that the dispersion pattern of the contaminants is not exceptional. There is a characteristic eastward spreading of pollution from the southwestern Baltic Sea, as the discharges in the main shipping lanes in the Baltic Proper are transported towards the eastern coast of the sea and northward. The wastewater from ship operations in the western Gulf of Finland and northern Baltic Proper is the source of contamination of the southeastern Gulf of Bothnia. Thus, the MPAs there could be impacted by the mixture of shipborne contaminants due to their dispersion by currents. The MPAs in the Danish Sounds, the southwestern Baltic Sea and the Gulf of Finland have the highest pressure by shipborne contaminants due to dense ship traffic and presence of harbors in the neighborhood.

The monitoring of shipborne contaminants close to the shipping lanes can be deceptive. Our study shows that the dispersion of the contaminants is rapid, i.e., about two days and everyday operational discharges of the ships do not leave detectable trails in the water. Indeed, if “a new” shipborne contaminant is introduced to the marine environment, the background concentration of which is much lower than the instantaneous loads, then the trail of higher concentration can be detectable for a longer period. Therefore, for experimental mapping of the marine area affected by different shipborne wastewater sources, we suggest using a marker chemical compound which is unique for the corresponding waste stream. Additionally, the contaminants that are discharged in particulate form or are absorbed by detritus and suspended particulate matter and settle in the water, form an elevated concentration area at the sea floor close to the shipping lane.

CRediT authorship contribution statement

Ilja Maljutenko: Methodology, Writing – original draft, Conceptualization, Visualization. **Ida-Maja Hassellöv:** Resources, Writing – review & editing, Conceptualization, Funding acquisition, Project administration. **Martin Eriksson:** Resources, Writing – review & editing, Project administration. **Erik Ytreberg:** Resources, Writing – review & editing. **Daniel Yngsell:** Resources. **Lasse Johansson:** Methodology, Writing – review & editing. **Jukka-Pekka Jalkanen:** Methodology, Writing – review & editing, Funding acquisition. **Mariliis Kõuts:** Resources, Writing – review & editing. **Mari-Liis Kasemets:** Resources, Writing – review & editing. **Jana Moldanova:** Writing – review & editing, Funding acquisition, Project administration. **Kerstin Magnusson:** Writing – review & editing, Funding acquisition. **Urmas Raudsepp:** Conceptualization, Writing – original draft, Funding acquisition.

Declaration of competing interest

The authors declare that they have no known competing financial interests or personal relationships that could have appeared to influence the work reported in this paper.

Acknowledgments

This research has been supported by the BONUS SHEBA project supported by BONUS (Art 185), funded jointly by the European Union, the Academy of Finland, Estonian Research Council, Swedish Agency for Marine and Water Management, Swedish Environmental Protection Agency and the Swedish Research Council for Environment, Agricultural Sciences and Spatial Planning (FORMAS) and Forschungszentrum Jülich

Beteiligungsgesellschaft mbH (Germany). We would also like to acknowledge the support from the European Union's Horizon 2020 research and innovation programme under grant agreement #874990 (EMERGE project). This work reflects only the authors' view and INEA is not responsible for any use that may be made of the information it contains. We are grateful to the HELCOM member states for allowing the use of HELCOM AIS data in this research. We are grateful to GETM, FABM community for the code development and maintenance. An allocation of computing time from the High Performance Computing cluster at the TalTech is gratefully acknowledged.

Appendix A

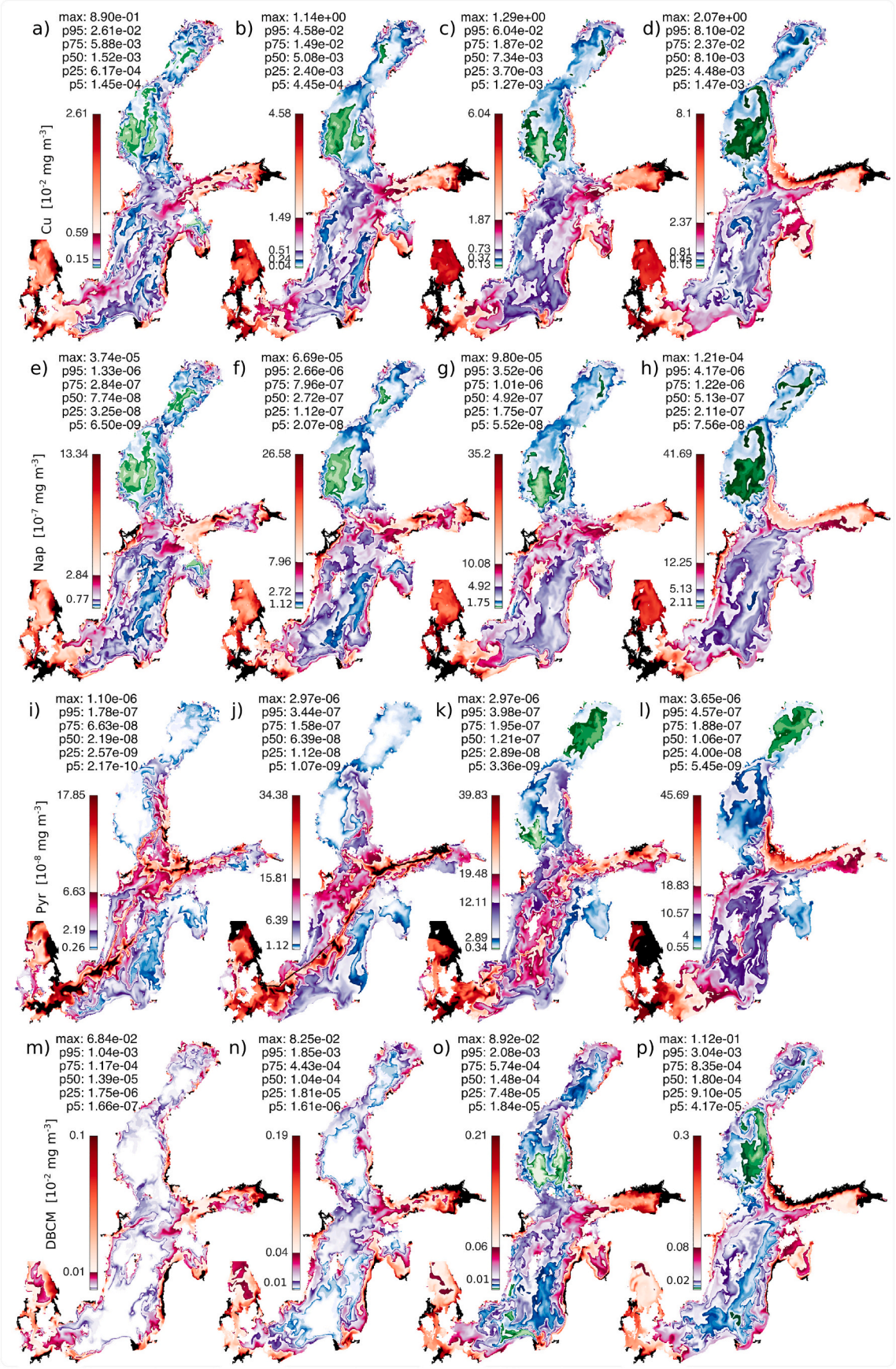

Fig. A1. The concentrations of copper, naphthalene, pyrene and dibromochloromethane (rows) at the surface by the end of the March, June, September and December 2012 (columns). Different color shades of green, blue, violet, pink and red show the ranges of 5th, 25th, 50th, 75th and 95th percentiles of the

concentrations, respectively. The values of percentiles are shown in each subplot.

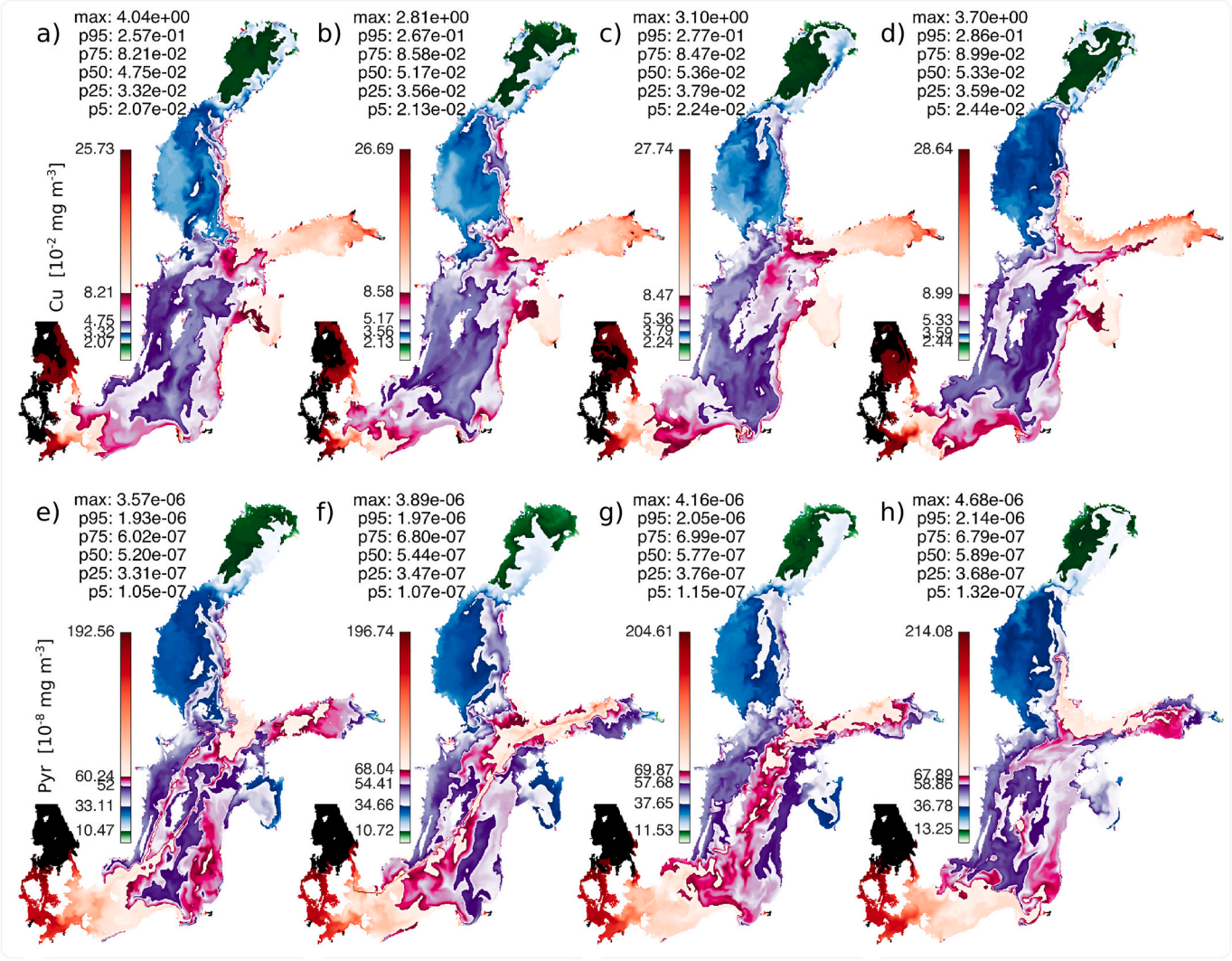

Fig. A2. The concentrations of copper and pyrene (rows) at the surface by the end of the March, June, September and December (columns) during the 5th year simulation. Different color shades of green, blue, violet, pink and red show the ranges of 5th, 25th, 50th, 75th and 95th percentiles of the concentrations, respectively. The values of percentiles are shown in each subplot.

References

Abioye, O.P., Loto, C.A., Fayomi, O.S.I., 2019. Evaluation of anti-biofouling progresses in marine application. J. Bio- Tribo-Corros. 5, 22. https://doi.org/10.1007/s40735-018-0213-5.

Almeida, E., Diamantino, T.C., de Sousa, O., 2007. Marine paints: the particular case of antifouling paints. Progress Org. Coat. 59 (1), 2–20. https://doi.org/10.1016/j.porgcoat.2007.01.017.

Altug, G., Gurun, S., Cardak, M., Ciftci, P.S., Kalkan, S., 2012. The occurrence of pathogenic bacteria in some ships' ballast water incoming from various marine regions to the sea of Marmara, Turkey. Mar. Environ. Res. 81, 35–42. https://doi.org/10.1016/j.marenvres.2012.08.005.

Andersson, K., Brynolf, S., Lindgren, J., Wilewska-Bien, M. (Eds.), 2016. Shipping and the Environment. Improving Environmental Performance in Marine Transportation. Springer, Berlin, Heidelberg. https://doi.org/10.1007/978-3-662-49045-7_9.

Bach, L.T., Riebesell, U., Sett, S., Febiri, S., Rzepka, P., Schulz, K.G., 2012. An approach for particle sinking velocity measurements in the 3–400 lm size range and considerations on the effect of temperature on sinking rates. Mar. Biol. 159, 1853–1864. https://doi.org/10.1007/s00227-012-1945-2.

Baumard, P., Budzinski, H., Garrigues, P., Dizer, H., Hansen, P.D., 1999. Polycyclic aromatic hydrocarbons in recent sediment and mussels (Mytilus edulis) from the Western Baltic Sea: occurrence, bioavailability and seasonal variations. Mar. Environ. Res. 47, 17–47. https://doi.org/10.1016/S0141-1136(98)00105-6.

Biziuk, M., 2001. Determination of selected anthropogenic organic compounds in southern Baltic. Anal. Lett. 34, 1517–1528. https://doi.org/10.1081/AL-100104924.

Blossom, N., 2002. Proceedings 11th International Congress on Marine Corrosion and Fouling. Session: Copper for Biofouling Control, July 22–26 2002, San Diego.

Bowen, H.J.M., 1985. The cycles of copper, silver and gold. In: Hutzinger, D. (Ed.), The Handbook of Environmental Chemistry. Vol. 1. Part D: The Natural Environment and Biogeochemical Cycles. Springer-Verlag, New York, pp. 1–26. https://doi.org/10.1007/978-3-540-39209-5-1.

Boxall, A.B.A., Comber, S.D., Conrad, A.U., Howcroft, J., Zaman, N., 2000. Inputs, monitoring and fate modelling of antifouling biocides in UK estuaries. Mar. Pollut. Bull. 40, 898–905. https://doi.org/10.1016/S0025-326X(00)00021-7.

Bravo-Linares, C.M., Mudge, S.M., Loyola-Sepulveda, R.H., 2007. Occurrence of volatile organic compounds (VOCs) in Liverpool Bay, Irish Sea. Mar. Pollut. Bull. 54, 1742–1753. https://doi.org/10.1016/j.marpolbul.2007.07.013.

Bruggeman, J., Bolding, K., 2014. A general framework for aquatic biogeochemical models. Environ. Model. Softw. 61, 249–265. https://doi.org/10.1016/j.envsoft.2014.04.002.

Burchard, H., Bolding, K., 2002. GETM – a general estuarine transport model. Scientific documentation.. In: Tech. Rep. EUR 20253 en.

Cheniti, R., Rochon, A., Frihi, H., 2018. Ship traffic and the introduction of diatoms and dinoflagellates via ballast water in the port of Annaba, Algeria. J. Sea Res. 133, 154–165. https://doi.org/10.1016/j.seares.2017.07.008.

Chu Van, T., Ramirez, J., Rainey, T., Ristovski, Z., Brown, R.J., 2019. Global impacts of recent IMO regulations on marine fuel oil refining processes and ship emissions. Transp. Res. Part D: Transp. Environ. 70, 123–134. https://doi.org/10.1016/j.trd.2019.04.001.

Claremar, B., Haglund, K., Rutgersson, A., 2017. Ship emissions and the use of current air cleaning technology: contributions to air pollution and acidification in the Baltic Sea. Earth System Dynamics 8 (4), 901–919. https://doi.org/10.5194/esd-8-901-2017.

David, M., Gollasch, S., 2008. EU shipping in the dawn of managing the ballast water issue. Mar. Pollut. Bull. 56, 1966–1972. https://doi.org/10.1016/j.marpolbul.2008.09.027.

Delacroix, S., Vogelsang, C., Tobiesen, A., Liltved, H., 2013. Disinfection by-products and ecotoxicity of ballast water after oxidative treatment - results and experiences from seven years of full-scale testing of ballast water management systems. Mar. Pollut. Bull. 73 (1), 24–36. https://doi.org/10.1016/j.marpolbul.2013.06.014.

Det Norske Veritas, 2009. Study on Discharge Factors for Legal Operational Discharge to Sea From Vessels in Norwegian Waters. Report No. 2009-0284, Rev. No. 2.

EU Directive 2008/105/EC. DIRECTIVE 2008/105/EC OF THE EUROPEAN PARLIAMENT AND OF THE COUNCIL of 16 December 2008 on environmental quality standards in the field of water policy, amending and subsequently repealing Council Directives 82/176/EEC, 83/513/EEC, 84/156/EEC, 84/491/EEC, 86/280/EEC and amending Directive 2000/60/EC of the European Parliament and of the Council.

DNV-GL, 2020. Alternative Fuels Insights. https://www.dnvgl.com/services/alternative-fuels-insight-128171. (Accessed 6 January 2020).

Döös, K., Meier, H.E.M., Döscher, R., 2004. The Baltic haline conveyor belt or the overturning circulation and mixing in the Baltic. Ambio 33, 261–266. https://doi.org/10.1579/0044-7447-33.4.261.

Endres, S., Maes, F., Hopkins, F., Houghton, K., Mårtensson, E.M., Oeffner, J., Quack, B., Singh, P., Turner, D., 2018. A new perspective at the ship-air-sea-interface: the environmental impacts of exhaust gas scrubber discharge. Front. Mar. Sci. 5, 139. https://doi.org/10.3389/fmars.2018.00139.

Endresen, Ø., Behrens, H.L., Brynestad, S., Andersen, A.B., Skjong, R., 2004. Challenges in global ballast water management. Mar. Pollut. Bull. 48, 615–623. https://doi.org/10.1016/j.marpolbul.2004.01.016.

Farrington, J.W., 2013. Oil pollution in the marine environment I: inputs, big spills, small spills, and dribbles. Environ. Sci. Policy Sustain. Dev. 55 (6), 3–13. https://doi.org/10.1080/00139157.2013.843980.

Feng, D., Chen, X., Tian, W., Qian, Q., Shen, H., Liao, D., Lv, B., 2017. Pollution characteristics and ecological risk of heavy metals in ballast tank sediment. Environ. Sci. Pollut. Res. 24 (4), 3951–3958. https://doi.org/10.1007/s11356-016-8113-z.

Fisher, D., Yonkos, L., Ziegler, G., Friedel, E., Burton, D., 2014. Acute and chronic toxicity of selected disinfection byproducts to Daphnia magna, Cyprinodon variegatus, and Isochrysis galbana. Water Res. 55, 233–244. https://doi.org/10.1016/j.watres.2014.01.056.

Gaylarde, C.C., Neto, J.A.B., da Fonseca, E.M., 2021. Paint fragments as polluting microplastics: a brief review. Mar. Pollut. Bull. 162, 111847 https://doi.org/10.1016/j.marpolbul.2020.111847.

GESAMP (IMO/FAO/UNESCO-IOC/UNIDO/WMO/IAEA/UN/UN Environment/UNDP/ISA Joint Group of Experts on the Scientific Aspects of Marine Environmental Protection), 2019. Methodology for the Evaluation of Ballast Water Management Systems Using Active Substances. Rep. Stud. GESAMP No. 101.

Geyer, B., 2014. High-resolution atmospheric reconstruction for Europe 1948–2012: coastDat2. Earth Syst. Sci. Data 6, 147–164. https://doi.org/10.5194/essd-6-147-2014.

Gräwe, U., Holtermann, P., Klingbeil, K., Burchard, H., 2015. Advantages of vertically adaptive coordinates in numerical models of stratified shelf seas. Ocean Model 92, 56–68. https://doi.org/10.1016/j.ocemod.2015.05.008.

Greer, C.D., Peter, V., Hodson, P.V., Li, Z., King, T., Lee, K., 2012. Toxicity of crude oil chemically dispersed in a wave tank to embryos of Atlantic herring (Clupea harengus). Environ. Toxicol. Chem. 31, 1324–1333. https://doi.org/10.1002/etc.1828.

Gubelit, Y., Polyak, Y., Dembska, G., Pazikowska-Sapota, G., Zegarowski, L., Kochura, D., Krivorotov, D., Podgornaya, E., Burova, O., Maazouzi, C., 2016. Nutrient and metal pollution of the eastern gulf of Finland coastline: sediments, macroalgae, microbiota. Sci. Total Environ. 550, 806–819. https://doi.org/10.1016/j.scitotenv.2016.01.122.

Guha, S., Peters, C.A., Jaffé, P.R., 1999. Multisubstrate biodegradation kinetics of naphthalene, phenanthrene, and pyrene mixtures. Biotechnol. Bioeng. 65 (5), 491–499. https://doi.org/10.1002/(SICI)1097-0290(19991205)65:5<491::AID-BIT1>3.0.CO;2-H.

Hall Jr., L.W., Anderson, R.D., 1999. A deterministic ecological risk assessment for copper in European saltwater environments. Mar. Pollut. Bull. 38 (3), 207–218. https://doi.org/10.1016/S0025-326X(98)00164-7.

Hassellöv, I.-M., Koski, M., Broeg, K., Marin-Enriquez, O., Tronczyński, J., Dulière, V., Murray, C., Bailey, S., Redfern, J., de Jong, K., Ponzevera, E., Belzunce-Segarra, M.J., Mason, C., Iacarella, J.C., Lyons, B., Fernandes, J.A., Parmentier, K., 2020. ICES viewpoint background document: impact from exhaust gas cleaning systems (scrubbers) on the marine environment (Ad hoc). ICES Sci. Rep. 2 (86), 40. https://doi.org/10.17895/ices.pub.7487.

He, Z., Liu, S.-S., Ni, J., Chen, Y., Yang, G.-P., 2019. Spatio-temporal variability and sources of volatile halocarbons in the South Yellow Sea and the East China Sea. Mar. Pollut. Bull. 149, 110583 https://doi.org/10.1016/j.marpolbul.2019.110583.

HELCOM, 2011. The fifth Baltic Sea pollution load compilation (PLC-5). Balt. Sea Environ. Proc. 128.

HELCOM, 2018. State of the Baltic Sea – second HELCOM holistic assessment 2011-2016. Balt. Sea Environ. Proc. 155.

Hermansson, A., Hassellöv, I.-M., Moldanová, J., Ytreberg, E., 2021. Comparing emissions of polyaromatic hydrocarbons and metals from marine fuels and scrubbers. Transp. Res. Part D: Transp. Environ. 97, 102912 https://doi.org/10.1016/j.trd.2021.102912.

Hodgkins, L.M., Mulligan, R.P., McCallum, J.M., Weber, K.P., 2019. Modelling the transport of shipborne per- and polyfluoroalkyl substances (PFAS) in the coastal environment. Sci. Total Environ. 658, 602–613. https://doi.org/10.1016/j.scitotenv.2018.12.230.

Hordoir, R., Meier, H.E.M., 2012. Effect of climate change on the thermal stratification of the Baltic Sea: a sensitivity experiment. Clim. Dyn. 38, 1703–1713. https://doi.org/10.1007/s00382-011-1036-y.

HVMFS, 2013. Havs- och vattenmyndighetens föreskrifter om klassificering och miljökvalitetsnormer avseende ytvatten. https://www.havochvatten.se/download/18.67e0eb431695d8639337366a/1552573474210/2013-19-keu-2019-01-01-ersatt-av-2019-25.pdf. (Accessed 6 January 2020).

IMO, 2001. International Convention on the Control of Harmful Anti-fouling Systems on Ships (AFS), 2001.

IMO, 2004. International Convention for the Control and Management of Ships' Ballast Water and Sediments (BWM), 2004.

IMO, 2011. International convention for the prevention of pollution from ships (MARPOL). In: Marpol: Articles, Protocols, Annexes, Unified Interpretations of the International Convention for the Prevention of Pollution from Ships, 1973, as Modified by the Protocol of 1978 Relating Thereto.

Jägerbrand, A.K., Brutemark, A., Svedén, J.B., Gren, I.-M., 2019. A review on the environmental impacts of shipping on aquatic and nearshore ecosystems. Sci. Total Environ. 695, 133637 https://doi.org/10.1016/j.scitotenv.2019.133637.

Jalkanen, J.-P., Brink, A., Kalli, J., Pettersson, H., Kukkonen, J., Stipa, T., 2009. A modelling system for the exhaust emissions of marine traffic and its application in the Baltic Sea area. Atmos. Chem. Phys. 9, 9209–9223. https://doi.org/10.5194/acp-9-9209-2009.

Jalkanen, J.-P., Johansson, L., Brink, A., Kalli, J., Kukkonen, J., Stipa, T., 2012. Extension of an assessment model of ship traffic exhaust emissions for particulate matter and carbon monoxide. Atmos. Chem. Phys. 12, 2641–2659. https://doi.org/10.5194/acp-12-2641-2012.

Jalkanen, J.-P., Johansson, L., Wilewska-Bien, M., Granhag, L., Ytreberg, E., Eriksson, K. M., Yngsell, D., Hassellöv, I.-M., Magnusson, K., Raudsepp, U., Maljutenko, I., Styhre, L., Winnes, H., Moldanova, J., 2021. Modeling of discharges from Baltic Sea shipping. Ocean Sci. 17 (3), 699–728. https://doi.org/10.5194/os-2020-99.

Jędrasik, J., Kowalewski, M., 2019. Mean annual and seasonal circulation patterns and long-term variability of currents in the Baltic Sea. J. Mar. Syst. 193, 1–26. https://doi.org/10.1016/j.jmarsys.2018.12.011.

Johansson, L., Jalkanen, J.-P., Kalli, J., Kukkonen, J., 2013. The evolution of shipping emissions and the costs of recent and forthcoming emission regulations in the northern European emission control area. Atmos. Chem. Phys. 13, 11375–11389. https://doi.org/10.5194/acp-13-11375-2013.

Johansson, L., Jalkanen, J.-P., Kukkonen, J., 2017. Global assessment of shipping emissions in 2015 on a high spatial and temporal resolution. Atmos. Environ. 167, 403–415. https://doi.org/10.1016/j.atmosenv.2017.08.042.

Johansson, L., Ytreberg, E., Jalkanen, J.-P., Fridell, Eb, Martin Eriksson, K., Lagerström, M., Maljutenko, I., Raudsepp, U., Fischer, V., Roth, E., 2020. Model for leisure boat activities and emissions - implementation for the Baltic Sea. Ocean Sci. 16, 1143–1163. https://doi.org/10.5194/os-16-1143-2020.

Jonson, J.E., Gauss, M., Jalkanen, J.-P., Johansson, L., 2019. Effects of strengthening the Baltic Sea ECA regulations. Atmos. Chem. Phys. 19, 13469–13487. https://doi.org/10.5194/acp-19-13469-2019.

Jonsson, P.R., Moksnes, P.-O., Corell, H., Bonsdorff, E., Nilsson Jacobi, M., 2020. Ecological coherence of marine protected areas: new tools applied to the Baltic Sea network. Aquat. Conserv. Mar. Freshwat. Ecosyst. 30 (4), 743–760. https://doi.org/10.1002/aqc.3286.

Kernan, M., 2015. Climate change and the impact of invasive species on aquatic ecosystems. Aquat. Ecosyst. Health Manag. 18, 321–333. https://doi.org/10.1080/14634988.2015.1027636.

Koski, M., Stedmon, C., Trapp, S., 2017. Ecological effects of scrubber water discharge on coastal plankton: potential synergistic effects of contaminants reduce survival and feeding of the copepod Acartia tonsa. Mar. Environ. Res. 129, 374–385. https://doi.org/10.1016/j.marenvres.2017.06.006.

Kremling, K., Pohl, C., 1989. Studies on the spatial and seasonal variability of dissolved cadmium, copper and nickel in Northeast Atlantic surface waters. Mar. Chem. 27, 43–60. https://doi.org/10.1016/0304-4203(89)90027-3.

Kremling, K., Streu, P., 2000. Further evidence for a drastic decline of potentially hazardous trace metals in Baltic Sea surface waters. Mar. Pollut. Bull. 40, 674–679. https://doi.org/10.1016/S0025-326X(99)00247-7.

Kremling, K., Streu, P., 2001. The behaviour of dissolved Cd, Co, Zn, and Pb in North Atlantic near-surface waters (301N/601W–601N/21W). Deep-Sea Res. I 48, 2541–2567. https://doi.org/10.1016/S0967-0637(01)00036-X.

Kyei, S.K., Darko, G., Akaranta, O., 2020. Chemistry and application of emerging ecofriendly antifouling paints: a review. J. Coat. Technol. Res. 17, 315–332. https://doi.org/10.1007/s11998-019-00294-3.

Lagerström, M., Ytreberg, E., 2021. Quantification of Cu and Zn in antifouling paint films by XRF. Talanta 223, 121820. https://doi.org/10.1016/j.talanta.2020.121820.

Leppäranta, M., Myrberg, K., 2009. Physical Oceanography of the Baltic Sea. Springer, Berlin, Heidelberg. https://doi.org/10.1007/978-3-540-79703-6.

Lindgren, J.F., Wilewska-Bien, M., Granhag, L., Andersson, K., Eriksson, K.M., 2016. Discharges to the sea. In: Andersson, K., Brynolf, S., Lindgren, J.F., Wilewska-Bien, M. (Eds.), Shipping and the Environment. Springer, Berlin, Heidelberg. https://doi.org/10.1007/978-3-662-49045-7_4.

Lips, U., Zhurbas, V., Skudra, M., Väli, G., 2016. A numerical study of circulation in the Gulf of Riga, Baltic Sea. Part I: whole-basin gyres and mean currents. Cont. Shelf Res. 112, 1–13. https://doi.org/10.1016/j.csr.2015.11.008.

Liu, Y.N., Yvon-Levis, S.A., Hu, L., Salisbury, J.E., O'Hern, J.E., 2011. CHBr 3, CH2Br2, and CHClBr2 in the U.S. coastal waters during the Gulf of Mexico and East Coast carbon cruise. J. Geophys. Res. 116, 1440–1450. https://doi.org/10.1029/2010JC006729.

Liu, S.-S., He, Z., Yang, G.-P., 2020. Bromoform, dibromochloromethane, and dibromomethane over the East China Sea and the western Pacific Ocean: oceanic emission and spatial variation. Chemosphere 257, 127151. https://doi.org/10.1016/j.chemosphere.2020.127151.

Lubecki, L., Szymczak-Zula, M., Kowalewska, G., 2006. Methylphenanthrenes in the southern Baltic as markers of petrogenic pollution. Oceanologia 48 (1), 73–86.

Magnusson, K., Jalkanen, J.-P., Johansson, L., Smailys, V., Telemo, P., Winnes, H., 2018. Risk assessment of bilge water discharges in two Baltic shipping lanes. Mar. Pollut. Bull. 126, 575–584. https://doi.org/10.1016/j.marpolbul.2017.09.035.

Maljutenko, I., Raudsepp, U., 2014. Validation of GETM model simulated long-term salinity fields in the pathway of saltwater transport in response to the Major Baltic Inflows in the Baltic Sea. In: 2014 IEEE/OES Baltic International Symposium (BALTIC 2014): 2014 IEEE/OES Baltic International Symposium, Tallinn, 24-27.04.2014. Institute of Electrical and Electronics Engineers (IEEE), pp. 23–31. https://doi.org/10.1109/BALTIC.2014.6887830.

Maljutenko, I., Raudsepp, U., 2019. Long-term mean, interannual and seasonal circulation in the Gulf of Finland — the wide salt wedge estuary or gulf type ROFI. J. Mar. Syst. 195, 1–19. https://doi.org/10.1016/j.jmarsys.2019.03.004.

Matthäus, W., 1984. Climatic and seasonal variability of oceanological parameters in the Baltic Sea. Beiträge zur Meereskunde 51, 29–49.

Matthiessen, P., Reed, J., Johnson, M., 1999. Sources and potential effects of copper and zinc concentrations in the estuarine waters of Essex and Suffolk, United Kingdom. Mar. Pollut. Bull. 38, 908–920. https://doi.org/10.1016/S0025-326X(99)00090-9.

Meier, H.E.M., 2007. Modeling the pathways and ages of inflowing salt- and freshwater in the Baltic Sea. Estuar. Coast. Shelf Sci. 74 (4), 717–734. https://doi.org/10.1016/j.Ecss.2007.05.019.

Merico, E., Cesari, D., Gregoris, E., Gambaro, A., Cordella, M., Contini, D., 2021. Shipping and air quality in Italian port cities: state-of-the-art analysis of available results of estimated impacts. Atmosphere 2021 (12), 536. https://doi.org/10.3390/atmos12050536.

Mestres, M., Sierra, J.P., Mösso, C., Sánchez-Arcilla, A., 2010. Modelling the sensitivity to various factors of shipborne pollutant discharges. Environ. Model Softw. 25, 333–343. https://doi.org/10.1016/j.envsoft.2009.08.006.

Moldanová, J., Hassellöv, I.-M., Matthias, V., Fridell, E., Jalkanen, J.-P., Ytreberg, E., Quante, M., Tröltzsch, J., Maljutenko, I., Raudsepp, U., Eriksson, K.M., 2021. Framework for the environmental impact assessment of operational shipping. Ambio. https://doi.org/10.1007/s13280-021-01597-9. In press.

Munari, C., Mistri, M., 2007. Effect of copper on the scope for growth of clams (Tapes philippinarum) from a farming area in the northern Adriatic Sea. Mar. Environ. Res. 64, 347–357. https://doi.org/10.1016/j.marenvres.2007.02.006.

Naik, R.K., Naik, M.M., D'Costa, P.M., Shaikh, F., 2019. Microplastics in ballast water as an emerging source and vector for harmful chemicals, antibiotics, metals, bacterial pathogens and HAB species: a potential risk to the marine environment and human health. Mar. Pollut. Bull. 149, 110525 https://doi.org/10.1016/j.marpolbul.2019.110525.

Parks, M., Ahmasuk, A., Compagnoni, B., Norris, A., Rufe, R., 2019. Quantifying and mitigating three major vessel waste streams in the northern Bering Sea. Mar. Policy 106, 103530. https://doi.org/10.1016/j.marpol.2019.103530.

Pohl, C., Hennings, U., 2005. The coupling of long-term trace metal trends to seasonal diffusive trace metal fluxes at the oxic-anoxic interface in the Gotland Basin; (57°19,20`N; 20°03,00E) Baltic Sea. J. Mar. Syst. 56, 207–225. https://doi.org/10.1016/j.jmarsys.2004.10.001.

Raudsepp, U., Laanemets, J., Maljutenko, I., Hongisto, M., Jalkanen, J.-P., 2013. Impact of ship-borne nitrogen deposition on the Gulf of Finland ecosystem: an evaluation. Oceanologia 55 (4), 837–857. https://doi.org/10.5697/oc.55-4.837.

Raudsepp, U., Maljutenko, I., Kõuts, M., Granhag, L., Wilewska-Bien, M., Hassellöv, I.-M., Eriksson, K.M., Johansson, L., Jalkanen, J.P., Karl, M., Matthias, V., Moldanova, J., 2019. Shipborne nutrient dynamics and impact on the eutrophication in the Baltic Sea. Sci. Total Environ. 671, 189–207. https://doi.org/10.1016/j.scitotenv.2019.03.264.

Raudsepp, U., Uiboupin, R., Laanemäe, K., Maljutenko, I., 2020. Geographical and seasonal coverage of sea ice in the Baltic Sea. In: Copernicus Marine Service Ocean State report, issue 4. J. Oper. Oceanogr. 13 (sup1), s111–s115. https://doi.org/10.1080/1755876X.2020.1785097.

Raudsepp, U., Männik, A., Maljutenko, I., Lagemaa, P., Rikka, S., Alari, V., Uiboupin, R., 2021. Extreme waves and low sea level during the storm in the Gulf of Bothnia, Baltic Sea. In: Copernicus Marine Service Ocean State Report, Issue 5. J. Oper. Oceanogr. 14 (sup1), s162–s173. https://doi.org/10.1080/1755876X.2021.1946240.

RIVM, 2012. Environmental risk limits for polycyclic aromatic hydrocarbons (PAHs). For direct aquatic, benthic, and terrestrial toxicity. RIVM report 607711007/2012. https://www.rivm.nl/bibliotheek/rapporten/607711007.pdf. (Accessed 6 January 2020).

Robinson, C.D., Webster, L., Martínez-Gómez, C., Burgeot, T., Gubbins, M.J., Thain, J.E., Vethaak, A.D., McIntosh, A.D., Hylland, K., 2017. Assessment of contaminant concentrations in sediments, fish and mussels sampled from the North Atlantic and European regional seas within the ICON project. Mar. Environ. Res. 124, 21–31. https://doi.org/10.1016/j.marenvres.2016.04.005.

Ruiz, G., Rawlings, T., Dobbs, F., Drake, L.A., Mullady, T., Huq, A., Colwell, R.R., 2000. Global spread of microorganisms by ships: ballast water discharged from vessels harbours a cocktail of potential pathogens. Nature 408, 49–50. https://doi.org/10.1038/35040695.

Sardain, A., Sardain, E., Leung, B., 2019. Global forecasts of shipping traffic and biological invasions to 2050. Nature Sustainability 2, 274–282. https://doi.org/10.1038/s41893-019-0245-y.

Schall, C., Heumann, K.G., Kirst, G.O., 1997. Biogenic volatile organoiodine and organobromine hydrocarbons in the Atlantic Ocean from 42° N to 72° S. Fresenius J. Anal. Chem. 359 (3), 298–305. https://doi.org/10.1007/s002160050577.

Settimo, G., Soggiu, M.E., Inglessis, M., Marsili, G., Avino, P., 2021. Persistent organic pollutants and metals in atmospheric deposition rates around the port-industrial area of Civitavecchia, Italy. Appl. Sci. (Switzerland) 11, 1–19. https://doi.org/10.3390/app11041827.

Soosaar, E., Maljutenko, I., Raudsepp, U., Elken, J., 2014. An investigation of anticyclonic circulation in the southern gulf of Riga during the spring period. Cont. Shelf Res. 78, 75–84. https://doi.org/10.1016/j.csr.2014.02.009.

Teuchies, J., Cox, T.J.S., Van Itterbeeck, K., Meysman, F.J.R., Blust, R., 2020. The impact of scrubber discharge on the water quality in estuaries and ports. Environ. Sci. Eur. 32 (1), 103. https://doi.org/10.1186/s12302-020-00380-z.

Thomas, K.V., Brooks, S., 2010. The environmental fate and effects of antifouling paint biocides. Biofouling 26, 73–88. https://doi.org/10.1080/08927010903216564.

Thor, P., Granberg, M.E., Winnes, H., Magnusson, K., 2021. Severe toxic effects on pelagic copepods from maritime exhaust gas scrubber effluents. Environ. Sci. Technol. 55 (9), 5826–5835. https://doi.org/10.1021/acs.est.0c07805.

Tiselius, P., Magnusson, K., 2017. Toxicity of treated bilge water: the need for revised regulatory control. Mar. Pollut. Bull. 114, 860–866. https://doi.org/10.1016/j.marpolbul.2016.11.010.

Torres, F.G., De-la-Torre, G.E., 2021. Environmental pollution with antifouling paint particles: distribution, ecotoxicology, and sustainable alternatives. Mar. Pollut. Bull. 169, 112529 https://doi.org/10.1016/j.marpolbul.2021.112529.

Turner, D.R., Hassellöv, I.-M., Ytreberg, E., Rutgersson, A., 2017. Shipping and the environment: smokestack emissions, scrubbers and unregulated oceanic consequences. Elementa 5, 45. https://doi.org/10.1525/elementa.167.

Uotila, P., Vihma, T., Haapala, J., 2015. Atmospheric and oceanic conditions and the extremely low Bothnian Bay sea ice extent in 2014/2015. Geophys. Res. Lett. 42, 7740–7749. https://doi.org/10.1002/2015GL064901.

Väli, G., Meier, H.E.M., Elken, J., 2013. Simulated halocline variability in the Baltic Sea and its impact on hypoxia during 1961–2007. J. Geophys. Res. Oceans 118 (12), 6982–7000. https://doi.org/10.1002/2013JC009192.

van Hattum, B., van Gils, J., Markus, A., Elzinga, H., Jansen, M., Baart, A., 2016. MAMPEC 3.1 Handbook. Technical Documentation. Deltares, Delft, The Netherlands.

von Schuckmann, K., Le Traon, P.-Y., Smith, N., Pascual, A., Brasseur, P., Fennel, K., Djavidnia, S., 2018. Copernicus marine Service Ocean state report, issue 2. J. Oper. Oceanogr. 11 (sup1), s1–s142. https://doi.org/10.1080/1755876X.2018.1489208.

Webb, A.L., Leedham-Elvidge, E., Hughes, C., Hopkins, F.E., Malin, G., Bach, L.T., Schulz, K., Crawfurd, K., Brussaard, C.P.D., Stuhr, A., Riebesell, U., Liss, P.S., 2016. Effect of ocean acidification and elevated fCO2 on trace gas production by a Baltic Sea summer phytoplankton community. Biogeosciences 13, 4595–4613. https://doi.org/10.5194/bg-13-4595-2016.

Werschkun, B., Banerji, S., Basurko, O.C., David, M., Fuhr, F., Gollasch, S., Grummt, T., Haarich, M., Jha, A.N., Kacan, S., Kehrer, A., Linders, J., Mesbahi, E., Pughiuc, D., Richardson, S.D., Schwarz-Schulz, B., Shah, A., Theobald, N., von Gunten, U., Wieck, S., Höfer, T., 2014. Emerging risks from ballast water treatment: the run-up to the international ballast water management convention. Chemosphere 112, 256–266. https://doi.org/10.1016/j.chemosphere.2014.03.135.

Westerlund, A., Tuomi, L., Alenius, P., Myrberg, K., Miettunen, E., Vankevich, R.E., Hordoir, R., 2019. Circulation patterns in the Gulf of Finland from daily to seasonal timescales. Tellus A 71 (1), 1627149. https://doi.org/10.1080/16000870.2019.1627149.

Wilewska-Bien, M., Granhag, L., Jalkanen, J.P., Johansson, L., Andersson, K., 2019. Phosphorus flows on ships: case study from the Baltic Sea. Proc. Inst. Mech. Eng. M 233 (2), 528–539. https://doi.org/10.1177/1475090218761761.

Witt, G., 1995. Polycyclic aromatic hydrocarbons in water and sediment of the Baltic Sea. Mar. Pollut. Bull. 31, 237–248. https://doi.org/10.1016/0025-326X(95)00174-L.

Wu, L., Xu, Y.-J., Wang, Q., Wang, F., Xu, Z., 2017. Mapping global shipping density from AIS data. J. Navig. 70, 67–81. https://doi.org/10.1017/S0373463316000345.

Ytreberg, E., Karlsson, J., Eklund, B., 2010. Comparison of toxicity and release rates of cu and zn from anti-fouling paints leached in natural and artificial brackish seawater. Sci. Total Environ. 408, 2459–2466. https://doi.org/10.1016/j.scitotenv.2010.02.036.

Ytreberg, E., Hassellöv, I.-M., Nylund, A.T., Hedblom, M., Al-Handal, A.Y., Wulff, A., 2019. Effects of scrubber washwater discharge on microplankton in the Baltic Sea. Mar. Pollut. Bull. 145, 316–324. https://doi.org/10.1016/j.marpolbul.2019.05.023.

Ytreberg, E., Eriksson, K.M., Maljutenko, I., Jalkanen, J.-P., Johansson, L., Hassellöv, I.-M., Granhag, L., 2020. Environmental impacts of grey water discharge from ships in the Baltic Sea. Mar. Pollut. Bull. 152, 110891 https://doi.org/10.1016/j.marpolbul.2020.110891.

Zaborska, A., Siedlewicz, G., Szymczycha, B., Dzierzbicka-Glowacka, L., Pazdro, K., 2019. Legacy and emerging pollutants in the Gulf of Gdańsk (southern Baltic Sea) – loads and distribution revisited. Mar. Pollut. Bull. 139, 238–255. https://doi.org/10.1016/j.marpolbul.2018.11.060.